

NERVA
IRRADIATION PROGRAM
Volume 1
GTR Test 18—Components Test

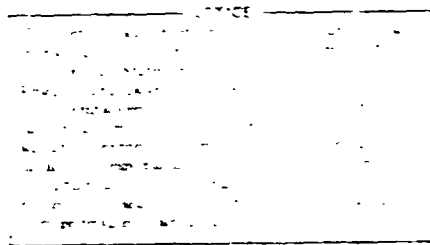
Form No AF 23 (607) 7-77

TECHNICAL DOCUMENT CENTER
Nuclear Rocket Operations

DOC. NO.

AGCS 0120-48

NUCLEAR AEROSPACE RESEARCH FACILITY



FZK-310-1
31 AUGUST 1966

NUCLEAR AEROSPACE RESEARCH FACILITY

**NERVA
IRRADIATION PROGRAM
Volume 1
GTR Test 18—Components Test**

J. W. Gurney
L. W. Neims

Prepared for
Space Nuclear Propulsion Office
of the
National Aeronautics and Space Administration
Cleveland, Ohio

Contract No. AF 29(601)-7077
Item 70

GENERAL DYNAMICS
Fort Worth Division

DISTRIBUTION OF THIS DOCUMENT UNLIMITED

FOREWORD

The test described in this document is designated SNPO-C, GTR-18. This is the twenty-first in a series of NERVA irradiation tests performed at the Nuclear Aerospace Research Facility (NARF) of the Fort Worth Division of General Dynamics Corporation for the Space Nuclear Propulsion Office, Cleveland, Ohio (SNPO-C). The 3-Mw Ground Test Reactor (GTR) and the 10-Mw Aerospace Systems Test Reactor (ASTR) are being used for these tests. Previous component tests were performed under Contract AF33(657)-7201 and AF29(601)-6213 and are reported in NARF Reports FZK-170, Vols. 1 through 8, and FZK-184, Vols. 1 through 6, respectively.

A materials test was also performed during this twenty-first NERVA irradiation test. This work is reported in Volume 2 of this series.

The test reported in this document was sponsored by the Aerojet-General Corporation and performed under Contract AF29(601)-7077.

SUMMARY

The fifteenth in the series of irradiation tests using the Ground Test Reactor at the Nuclear Aerospace Research Facility (NARF) to determine the effects of reactor radiation on candidate NERVA components and materials was concluded on 2 July 1966. The test was designated GTR 18. The test item was resistance temperature transducers. A measurement of the conversion of parahydrogen to orthohydrogen was also made.

The test conditions and subsequent results are described briefly below.

Resistance Temperature Transducers (RTT's)

Twenty RTT's with various shielding configurations covering their platinum elements were irradiated while submerged in liquid hydrogen. They were exposed to integrated neutron fluxes ranging from 1.50×10^{16} to 1.92×10^{16} n/cm² (E > 2.9 Mev) and gamma doses ranging from 1.8×10^{11} to 2.3×10^{11} ergs/gm(C). The average maximum temperature deviation, taken with the reactor retracted, for each type of RTT was as follows:

<u>Type RTT</u>	<u>Shielding</u>	<u>No. Irradiated</u>	<u>Avg Temp Deviation (°R)</u>
Rosemount 134EB186	Cadmium	2	1.37
Rosemount 134EB186	Hafnium	2	1.32
Rosemount 134EB186	Hafnium-Cadmium	3	1.42
Rosemount 134EB186	Stainless Steel	2	1.46
Rosemount 134EB186	None	2	1.52
Rosemount 134EB1X	None	2	1.48
Rosemount 134EB2X	None	2	1.40
Rosemount 137CJ	None	2	1.24

<u>Type RTT</u>	<u>Shielding</u>	<u>No. Irradiated</u>	<u>Avg Temp Deviation (°R)</u>
Rosemount 134EB250	None	1	1.58
Rosemount 110AA	None	1	4.57
Temtech 1881-2	None	1	Not Computed

A definite decrease in temperature deviation for all the RTT's one fifth of the way through the test can be attributed to loss of LH₂ flow over a 3-hr period.

Conversion of Parahydrogen to Orthohydrogen

A maximum of 3% conversion of parahydrogen to orthohydrogen was measured at the steady state. The conversion was observed to be related to nuclear radiation, and the mechanism appears to be associated with the liquid as well as the gas phase.

TABLE OF CONTENTS

	<u>Page</u>
FOREWORD	iii
SUMMARY	v
LIST OF FIGURES	ix
LIST OF TABLES	xiii
I. INTRODUCTION	1
II. EXPERIMENTAL ARRANGEMENT	3
III. RESISTANCE TEMPERATURE TRANSDUCERS	15
3.1 Experimental Procedure	15
3.2 Test Method	15
3.3 Data Presentation	16
3.3.1 Indicated Temperature	19
3.3.2 Reference Temperature	19
3.4 Discussion	20
IV. PARAHYDROGEN-ORTHOHYDROGEN CONVERSION	49
4.1 Purpose	49
4.2 Discussion	49
4.3 Experimental Setup	52
4.3.1 Gas Analyzer	52
4.3.2 Sample System	53

TABLE OF CONTENTS (cont'd)

	<u>Page</u>
4.4 Results	56
4.4.1 Maximum Conversion	56
4.4.2 Rise Time	56
4.4.3 Radiation Dependence	57
4.4.4 Dewar Charge-Rate Dependence	57
4.5 Conclusions	58
APPENDIX A. GTR RADIATION EFFECTS TESTING SYSTEM	61
APPENDIX B: DOSIMETRY TECHNIQUES AND DATA	67
APPENDIX C: EXCERPTS FROM REACTOR OPERATIONS LOG	79
REFERENCES	83
DISTRIBUTION	85

LIST OF FIGURES

<u>Figure</u>	<u>Page</u>
2-1 Instrumentation System	6
2-2 Pressure Measuring Instrumentation	7
2-3 Absolute Pressure Gage and Temperature Recorder	8
2-4 RTT Mounting Panel Locations Viewed from Reactor	9
2-5 RTT Mounting Panel (Location of Specific RTT's not Finalized)	10
2-6 RTT Test Fixture	11
2-7 Upper Portion of Assembly with Shroud Removed	12
2-8 RTT Test Fixture (After Irradiation)	13
2-9 Effluent Hydrogen Gas Analysis Setup	14
3-1 RTT Calibration Circuit	26
3-2 Block Diagram for RTT Test	27
3-3 Temperature Deviation vs Radiation Exposure: RTT 1 (Rosemount 134EB186, S/N 8927), Cadmium Shielded	28
3-4 Temperature Deviation vs Radiation Exposure: RTT 2 (Rosemount 134EB186, S/N 12325), Cadmium Shielded	29
3-5 Temperature Deviation vs Radiation Exposure: RTT 3 (Rosemount 134EB186, S/N 6317), Hafnium-Cadmium Shielded	30
3-6 Temperature Deviation vs Radiation Exposure: RTT 4 (Rosemount 134EB186, S/N 12330), Hafnium-Cadmium Shielded	31
3-7 Temperature Deviation vs Radiation Exposure: RTT 5 (Rosemount 134EB186, S/N 4092), Hafnium Shielded	32

LIST OF FIGURES (cont'd)

<u>Figure</u>		<u>Page</u>
3-8	Temperature Deviation vs Radiation Exposure: RTT 6 (Rosemount 134EB186, S/N 12340), Hafnium Shielded	33
3-9	Temperature Deviation vs Radiation Exposure: RTT 7 (Rosemount 134EB186, S/N 4094)	34
3-10	Temperature Deviation vs Radiation Exposure: RTT 8 (Rosemount 134EB186, S/N 4096), Stainless-Steel Shielded	35
3-11	Temperature Deviation vs Radiation Exposure RTT 9 (Rosemount 134EB186, S/N 4104)	36
3-12	Temperature Deviation vs Radiation Exposure: RTT 10 (Rosemount 134EB186, S/N 6319), Stainless Steel Shielded	37
3-13	Temperature Deviation vs Radiation Exposure: RTT 11 (Rosemount 134EB186, S/N 7365), hafnium-Cadmium Shielded	38
3-14	Temperature Deviation vs Radiation Exposure: RTT 12 (Rosemount 134EB1X, S/N 9372)	39
3-15	Temperature Deviation vs Radiation Exposure: RTT 13 (Rosemount 134EB2X, S/N 9371)	40
3-16	Temperature Deviation vs Radiation Exposure: RTT 14 (Rosemount 134EB2X, S/N 9370)	41
3-17	Temperature Deviation vs Radiation Exposure: RTT 15 (Rosemount 137CJ, S/N 1667)	42
3-18	Temperature Deviation vs Radiation Exposure: RTT 16 (Rosemount 137CJ, S/N 1666)	43
3-19	Percent Resistance Change vs Radiation Exposure: RTT 17 (Temtech 1881-2, S/N 6149)	44

LIST OF FIGURES (cont'd)

<u>Figure</u>	<u>Page</u>
3-20 Temperature Deviation vs Radiation Exposure: RTT 18 (Rosemount 134EB250, S/N 4107)	45
3-21 Temperature Deviation vs Radiation Exposure: RTT 19 (Rosemount 110AA, S/N 211)	46
3-22 Temperature Deviation vs Radiation Exposure: RTT 20 (Rosemount 134EB1X, S/N 9373)	47
4-1 Apogee General Purpose Gas Analysis System (AGPGAS)	59
4-2 Schematic of Effluent Gas Sampling System	60
A-1 Plan View of GTR Radiation Effects Testing System and Adjacent Reactor Control Room	63
A-2 Cutaway View of GTR Radiation Effects System	64
A-3 Irradiation Test Cell and Reactor Tank	65
B-1 Analytical GTR Neutron Spectrum	72
B-2 Location of Dosimetry Packets	73
B-3 Location of Dosimetry Packets, Groups 1 and 3	74
B-4 Dosimetry Packets, Group 1, Viewed from Reactor	75
B-5 Dosimetry Packets, Group 2, Facing Away from Reactor	76
B-6 Dosimetry Packets, Group 3, Facing Away from Reactor	77

LIST OF TABLES

<u>Table</u>		<u>Page</u>
3-1	Resistance Temperature Transducers	17
3-2	R_p and $\frac{dT}{dR}$ for Each RTT	20
B-1	Dosimetry Data (Measured)	68
B-2	RTT Exposure	69

I. INTRODUCTION

A series of tests is being performed at the Nuclear Aerospace Research Facility (NARF) of General Dynamics, Fort Worth Division, to determine the effects of nuclear radiation on components and materials proposed for use in the NERVA engines. Aerojet-General Corporation has prime responsibility for development of the NERVA engine.

This report deals with the fifteenth irradiation, designated GTR-13, of the series performed with the Ground Test Reactor (GTR). This test was performed in accordance with test specifications submitted by Aerojet-General Corporation (AGC), Azusa, California (Ref. 1). The test components were furnished by AGC and Los Alamos Scientific Laboratory (LASL). The parahydrogen-orthohydrogen gas analysis system was furnished by the National Bureau of Standards (NBS).

This report is divided into two parts. The first part deals with 20 resistance temperature transducers (RTT); the second, with the measurement of the para-ortho composition of hydrogen gas evolved from the liquid during the irradiation.

BLANK PAGE

II. EXPERIMENTAL ARRANGEMENT

In the GTR Radiation-Effects Testing System at NARF, components can be placed on test pallets or in controlled environmental chambers and positioned on the north, east, or west sides of the reactor. Photographs and a brief description of this facility are included in Appendix A. A more complete description may be found in Reference 2.

The east irradiation position was utilized in this experiment. An AGC-designed hydrogen dewar installed in that position contained the RTT's in a liquid-hydrogen (LH_2) environment and provided the source of irradiated hydrogen for the parahydrogen-to-orthohydrogen conversion measurement. The RTT test assembly was connected to instrumentation (Figs. 2-1, 2-2, and 2-3) in the control room by means of electrical harnesses and pneumatic lines approximately 120 ft long. The layout of the RTT box is shown in Figures 2-4 and 2-5.

The liquid-hydrogen test assembly that contained the 20 RTT's is shown in Figure 2-6. The upper portion of the assembly was enclosed in a shroud that was purged continuously with helium gas flowing at a rate of 0.5 cfm. This upper portion is shown with the shroud removed in Fig. 2-7. The lower portion consists of a sealed fixture attached to metal pipes welded to the underside of the shroud plate. Instrumentation harnesses pass through the pipes to the RTT's mounted inside

the fixture. The RTT's extended outward into the LH₂ container and were sealed to the fixture with K-seals. The RTT test fixture is shown in Figure 2-8.

The shroud exhaust was routed through a check valve at the top of the shroud and vented through a vent stack located at the north end of the facility. A burst disc was incorporated in the dewar and ported to the shroud exhaust for venting out of the pool. Normal hydrogen exhaust was vented from the dewar to the ASTR burn stack. The portion of exhaust required for the conversion measurement was tapped off this main exhaust system (Fig. 4-2) and run to the Effluent Hydrogen Gas Analysis Setup, shown in Figure 2-9. All exhaust fittings and the burst disc was enclosed in the shroud. Liquid hydrogen was supplied to the dewar through a vacuum-insulated, flexible transfer line. All electrical wiring was routed out of the dewar and shroud by means of hermetic connectors.

A liquid level system was incorporated to continuously monitor and control the liquid level in the dewar. A probe consisting of seven resistors and three thermocouples was used with an indicator panel which indicated the liquid level in the dewar. The three thermocouples were used in conjunction with Bristol control units to control the level in the dewar and to read out the temperature inside the dewar during warm-up.

Standard dosimetry techniques were used in measuring the integrated neutron fluxes and gamma doses to which the test

items were exposed. The application of these techniques in determining the radiation exposure is discussed in Appendix B.

During the irradiation, it was discovered that several of the RTT's had abnormally high resistance readings at 3-Mw power level as a result of gamma heating. A procedure of retracting the reactor every 6 hr was initiated to provide data unaffected by gamma heating. Half way through the test, this period of retraction was changed to one every 4 hr. After approximately 500 Mw-hr, the retractions were halted altogether because of problems with the reactor traversing mechanism.

The data plotted for RTT's were taken only during the periods when the reactor was retracted.

NPC 24,367
31-8693

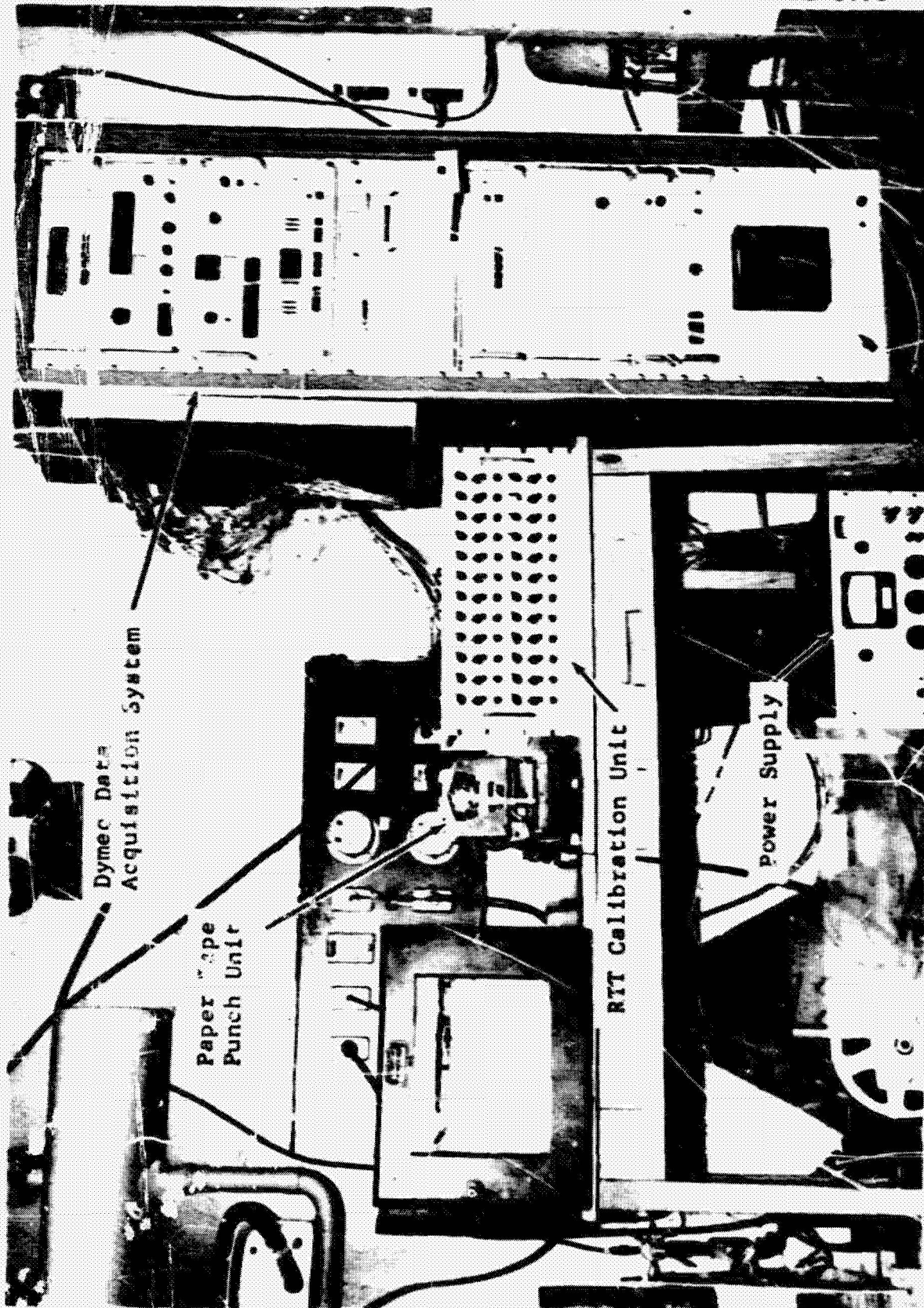


Figure 2-1 Instrumentation System

NPC 24,368
31-8696

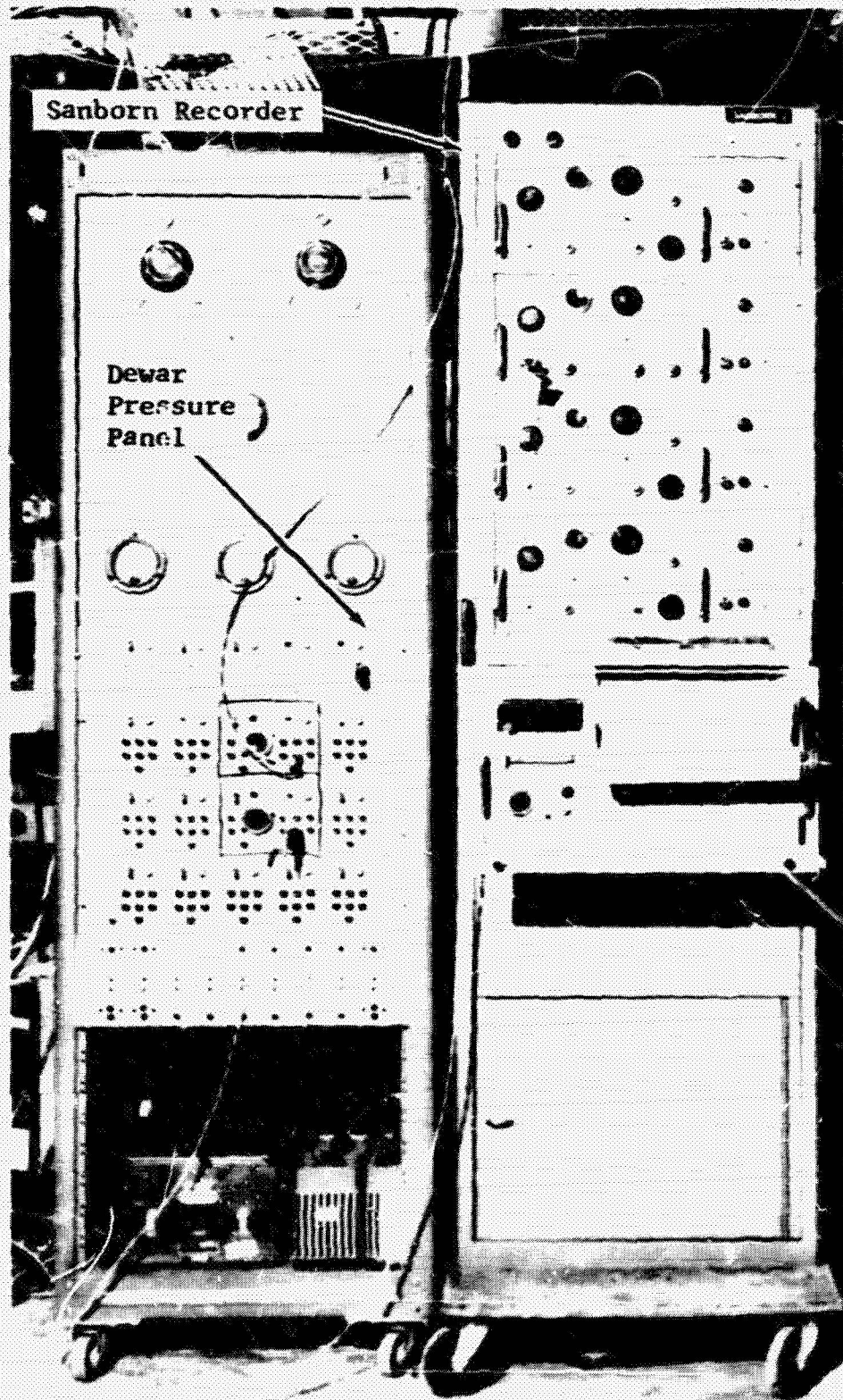


Figure 2-2 Pressure Measuring Instrumentation

NPC 24,369
31-8694

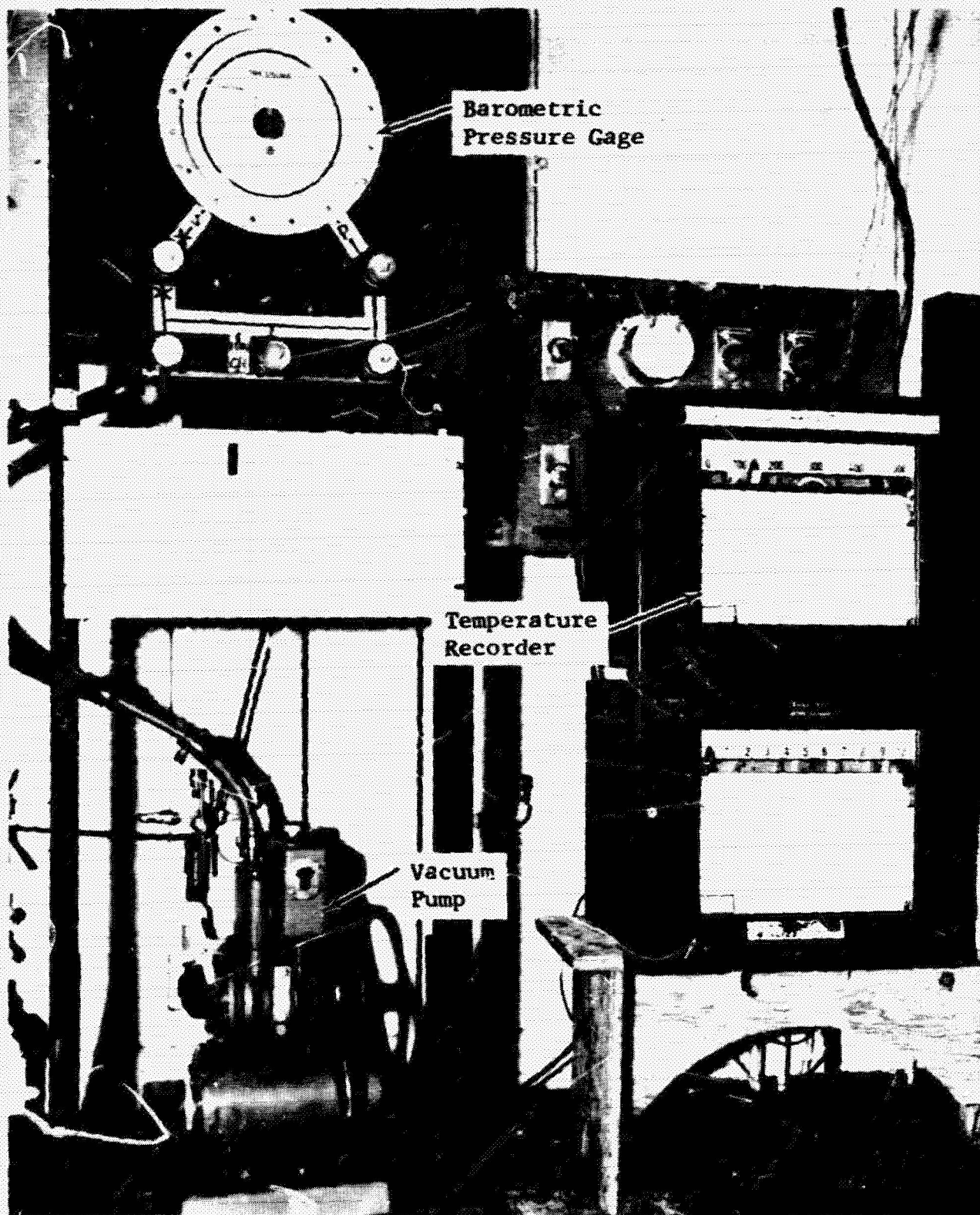


Figure 2-3 Absolute Pressure Gage and Temperature Recorder

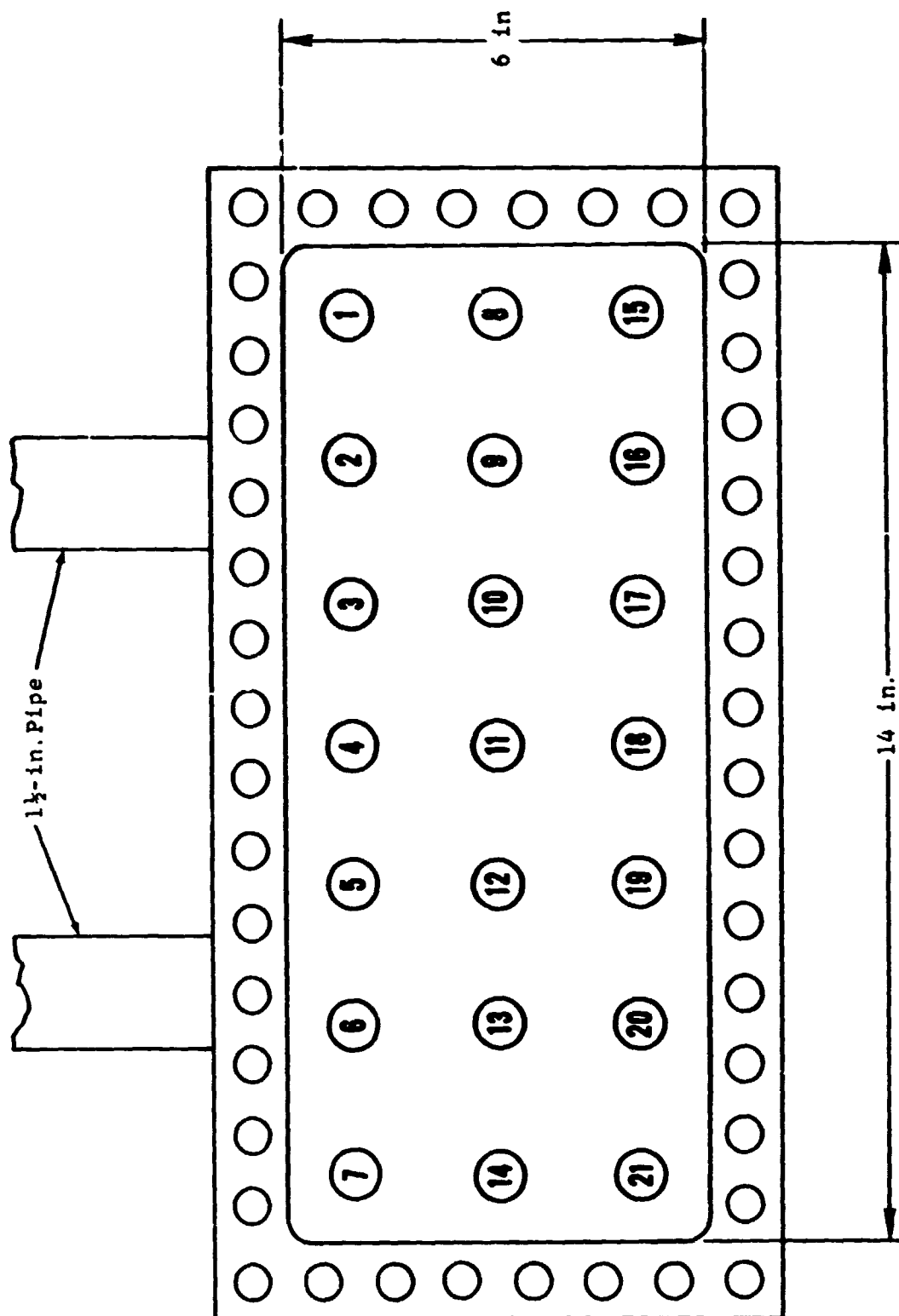


Figure 2-4 RTT Mounting-Panel Locations Viewed From Reactor

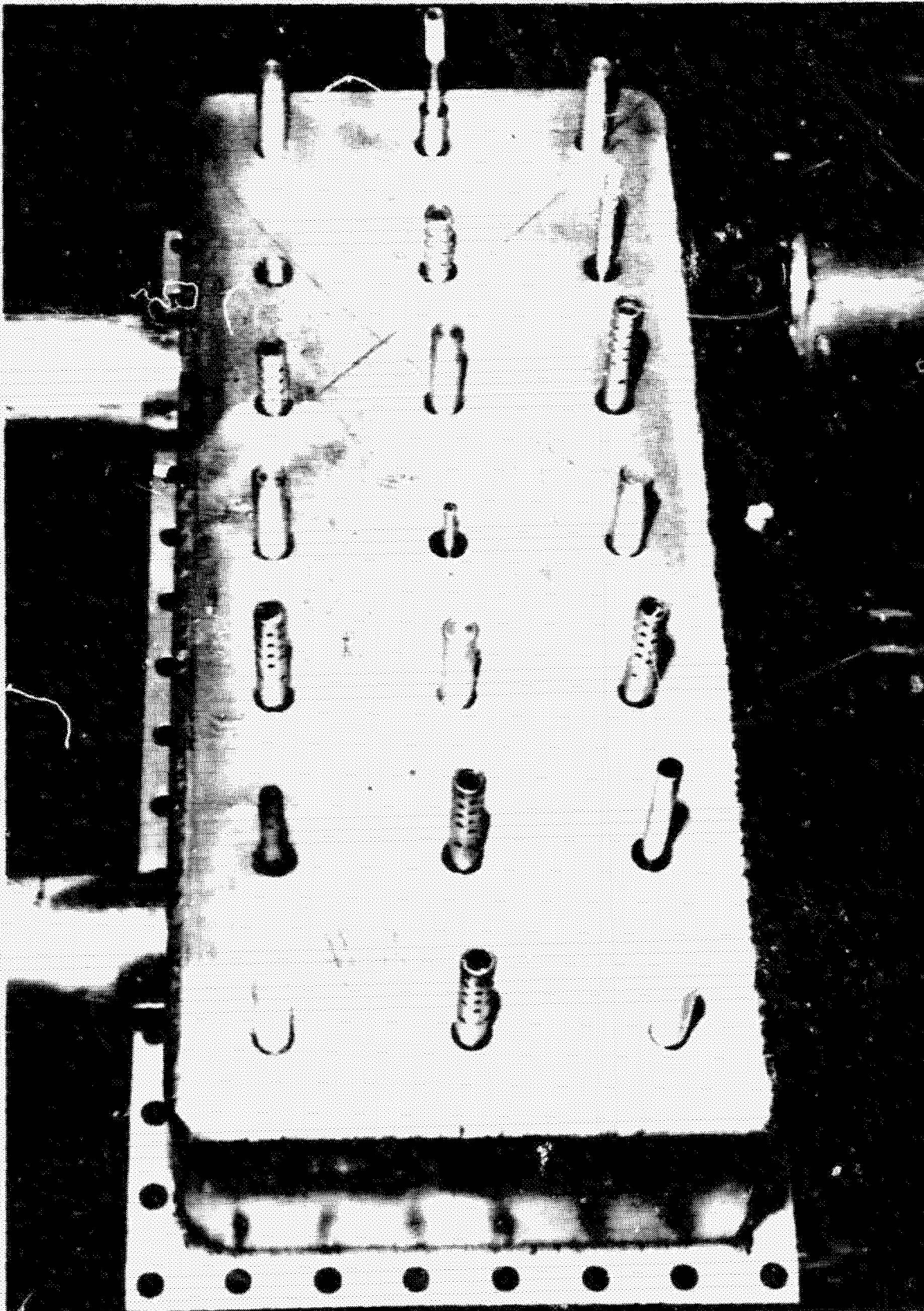


Figure 2-5 RTT Mounting Panel (Location of Specific RTT's Not Finalized)

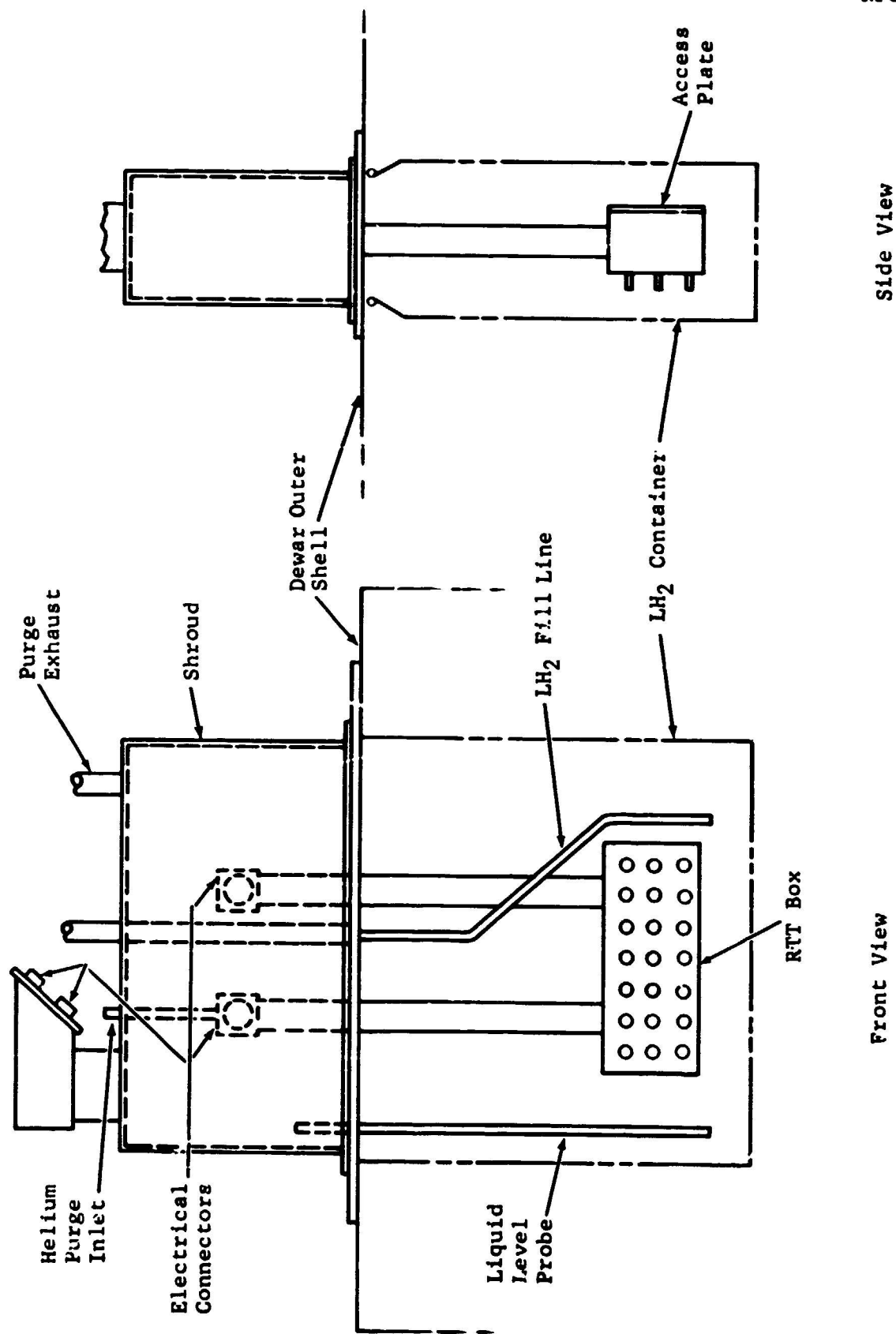


Figure 2-6 RTT Test Fixture

NPC 24,373
31-8654

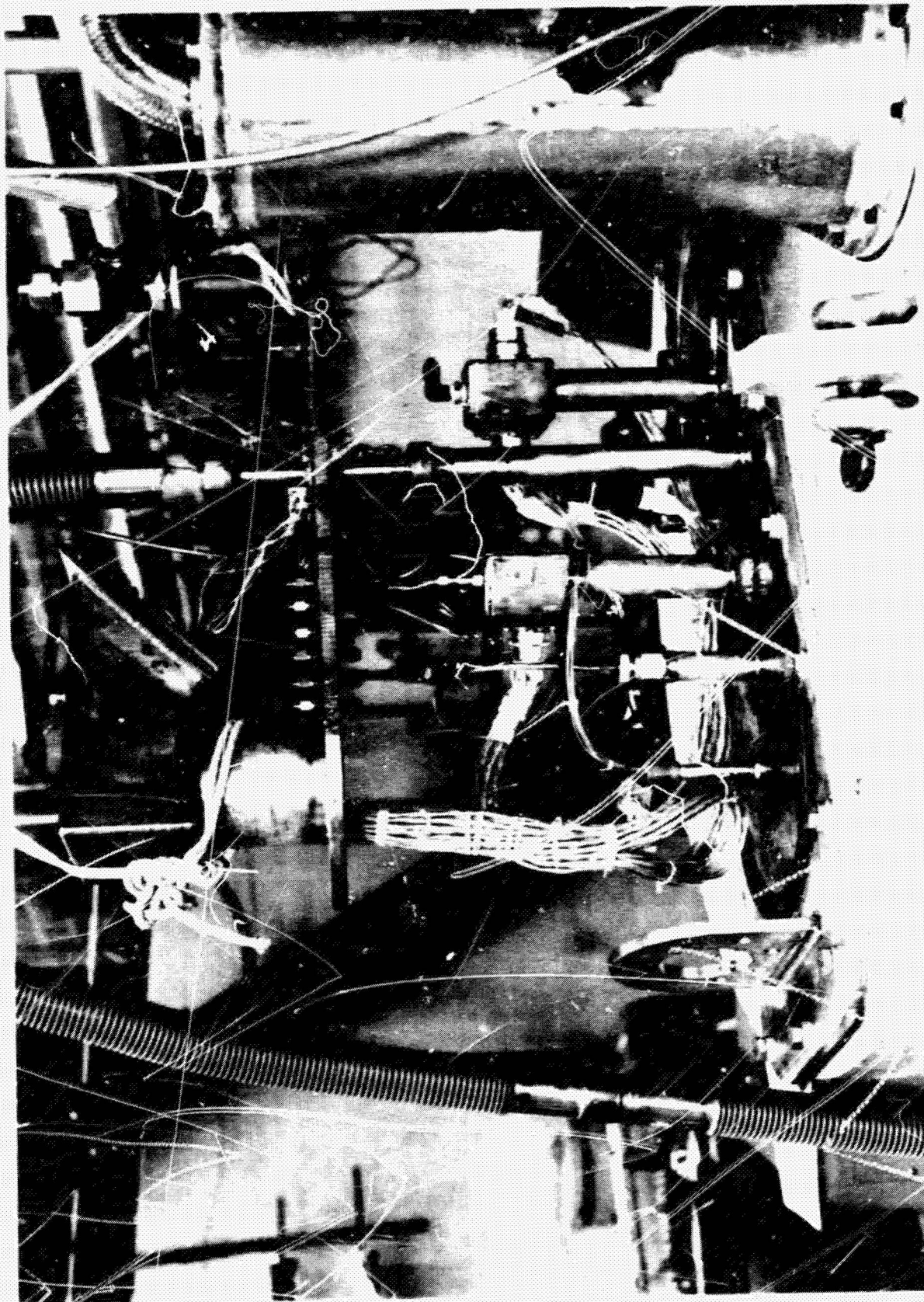


Figure 2-7 Upper Portion of Assembly With Shroud Removed

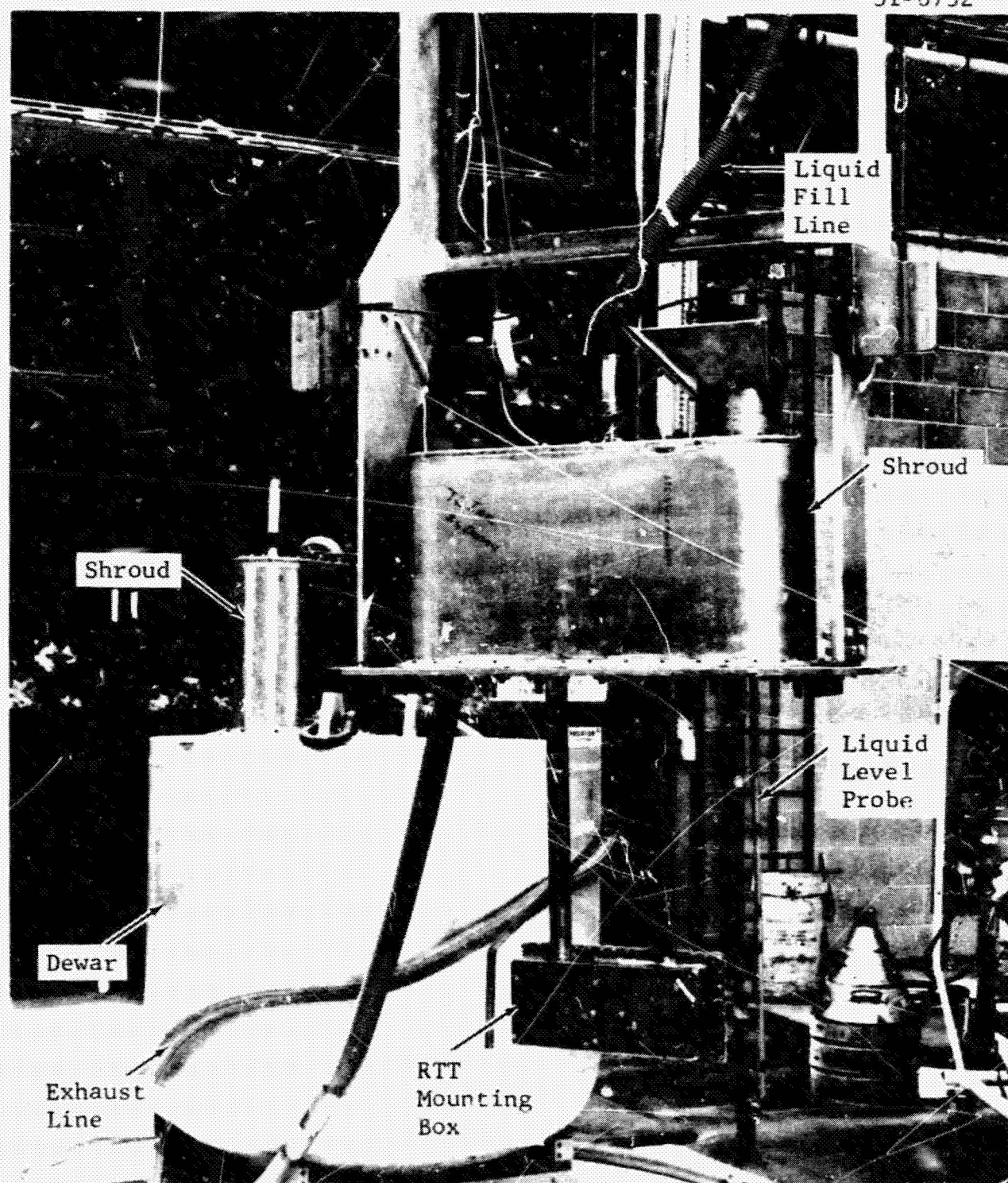


Figure 2-8 RTT Test Fixture (After Irradiation)

NPC 24,375
31-8695

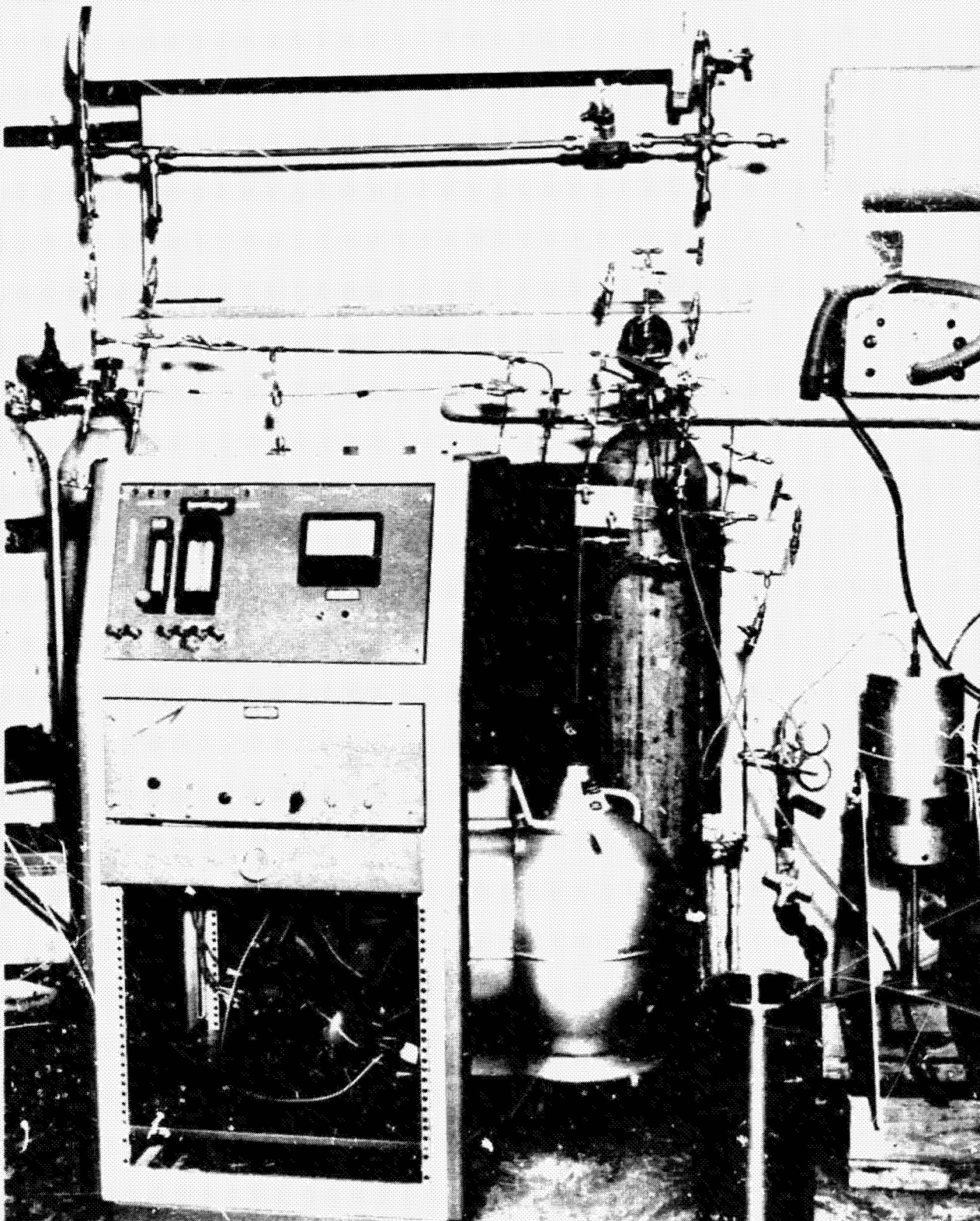


Figure 2-9 Effluent-Hydrogen Gas Analysis Setup

III. RESISTANCE TEMPERATURE TRANSDUCER

3.1 Experimental Procedure

Before the test setup was moved to the reactor area, data were recorded at room temperature, ice temperature, and liquid-nitrogen (LN_2) temperature with the same harness and instrumentation that would be used in the test. This procedure was repeated after the test setup was moved to the reactor area.

After irradiation was started, data cycles were taken with the reactor level at 1 Mw, again at 2 Mw, and finally at 3 Mw.

3.2 Test Method

Data were obtained from 20 resistance temperature transducers (RTT's) during the irradiation. These components are listed in Table 3-1.

The test components were held at LN_2 temperature during the 600-Mw-hr irradiation by maintaining the LN_2 level above the upper-most test component.

An AGC-furnished calibration panel - F/N 248428 - was used to connect the RTT's to a regulated 150-vdc power supply and to the digital data-acquisition system (Dymec 2010-D). A constant current was passed through each RTT and the voltage drop across each unit was measured, thus allowing the resistance of each unit to be determined. Adjustment of the calibration circuit for the RTT's was performed by monitoring the voltage across

the calibration resistor and adjusting the voltage to pre-specified values (Fig. 3-1).

The RTT and calibration resistor outputs were recorded on punched and printed tape. Adjustments were made as needed to maintain a constant current through each RTT. A block diagram for the RTT test is shown in Figure 3-2.

Prior to irradiation, the test components were submerged in LN_2 the excitation currents were adjusted, and 10 test cycles were made. These data yielded the necessary information for establishing the base-line data utilized to determine reference temperature and resistances for each RTT (see Section 3.3).

Data were gathered at reactor power levels of 1, 2, and 3 Mw. Data were gathered throughout the 3-Mw irradiation period at 1-hr intervals and for several hours after reactor shutdown.

Since the temperature of LN_2 is pressure-sensitive, the vapor pressure above the liquid was measured. To do this, a CEC Type 4-312-0002 pressure transducer of range ± 5 psid was used, along with an absolute barometric dial gage indicator. These pressures were used to determine the actual temperature for comparison with the temperatures indicated by the test items (see Section 3.3).

3.3 Data Presentation

A thorough analysis of all the data is not attempted in this report. Computer reduction of the data is being performed

Table 3-1
Resistance Temperature Transducers

RTT No.	Pro- vided by	Serial No.	Type*	Shielding Material	Loca- tion in Mount- ing Pencil	Constant Current (ma)
1	AGC	8927	134EB186	Cadmium	10	4.5
2	AGC	12333	134EB186	Cadmium	12	4.5
3	AGC	6317	134EB186	Hafnium-Cadmium	7	4.5
4	AGC	12330	134EB186	Hafnium-Cadmium	15	4.5
5	AGC	4092	134EB186	Hafnium	1	4.5
6	AGC	12340	134EB186	Hafnium	21	4.5
7	AGC	4094	134EB186	None	9	4.5
8	AGC	4096	134EB186	Stainless-Steel	18	4.5
9	AGC	4104	134EB186	None	3	4.5
10	AGC	6319	134EB186	Stainless-Steel	4	4.5
11	AGC	7365	134EB186	Hafnium-Cadmium	11	4.5
12	AGC	9372**	134EB1X	None	5	1
13	AGC	9371**	134EB2X	None	13	1
14	AGC	9370**	134EB2X	None	14	1
15	LASL	1667	137CJ	None	16	10
16	LASL	1666	137CJ	None	6	10
17	LASL	6149	1881-2	None	20	1
18	AGC	4107**	134EB250	None	17	1
19	AGC	211**	110AA	None	8	1
20	AGC	9373**	134EB1X	None	19	1

*All are Rosemount except RTT No. 17 (S/N 6149), which is Temtech.

**Previously irradiated in GTR Test 15 (Ref. 3).

at AGC and final results are not yet available. Therefore, the data presented here represents only a small portion of the total data. However, an effort was made to choose representative points, so that the curves presented here will closely resemble the finalized computer results.

The temperature deviation of the RTT's - that is, the difference between the indicated temperature of the RTT's and the actual temperature of the LH_2 - is plotted as a function of radiation exposure in megawatt-hours and neutron and gamma flux in Figures 3-3 through 3-22. The dose-rate effect of the RTT's was eliminated by plotting only the data taken with the reactor retracted. The temperature deviation at 600 Mw-hr for the 134EB RTT's ranged from 1.2° to 1.6°R . Among the previously irradiated RTT's, the 110AA had the highest temperature deviation at 600 Mw-hr, namely, 4.6°R . Since one of the LASL supplied transducers - Temtech S/N 6149 - did not have sufficient calibration information supplied with it to calculate temperature deviation, its plot is shown in terms of percent resistance change vs radiation exposure (Fig. 3-19).

Appendix C contains the reactor log for the irradiation.

The temperature deviation, T_D , is given as

$$T_D = T_I - T_R$$

where T_I is the temperature indicated by the RTT's and T_R the actual temperature of the LH_2 , or reference temperature.

3.3.1 Indicated Temperature

The slope of each RTT was determined from initial calibrations of the RTT's in LH_2 and liquid neon. An analysis of the test data showed that in every case the temperature indicated by the RTT's was higher than the preirradiation temperature, which was 36.3685°K . The slope

$$m = \frac{dT}{dR} = \frac{T_I - T_P}{R - R_P}$$

is slightly different for each RTT, even though many of the RTT's are of the same type.

Rearranging the slope equation gives

$$\begin{aligned} T_I &= m(R - R_P) + T_P \\ &= \frac{dT}{dR} (R - R_P) + T_P \end{aligned}$$

where $T_P = 36.3685^\circ\text{K}$, and R is the RTT resistance, R_P is the preirradiation resistance for each RTT, and R_P and $\frac{dT}{dR}$ differ for each RTT, as shown in Table 3-2.

3.3.2 Reference Temperature

The reference temperature is the temperature of the LH_2 surrounding the RTT's. With the assumption that the parahydrogen is at its boiling point throughout its volume, the reference temperature can be determined as a function of the dewar pressure.

Table 3-2

R_p and $\frac{dT}{dR}$ for Each RTT

RTT	R_p (ohms)	$\frac{dT}{dR}$ ($^{\circ}R/ohm$)
1	6.5118	1.0588
2	6.7641	1.1803
3	6.5522	1.1438
4	6.7094	1.1706
5	6.5654	1.1537
6	6.7039	1.1659
7	6.7558	1.1579
8	6.7280	1.1557
9	6.6731	1.1440
10	6.6440	1.1473
11	6.4738	1.1541
12	3.3100	2.4576
13	0.6389	1.1977
14	0.6120	10.620
15	0.2164	24.100
16	0.2171	24.117
17	1.0890	*
18	7.7296	1.1564
19	3.1999	3.7574
20	3.0897	2.3780

*Sufficient data not available to evaluate $\frac{dT}{dR}$ for this RTT.

From the experimental data, it was observed that the absolute pressure of the hydrogen (dewar pressure plus atmospheric pressure) varied by a few tenths of a pound, around 14.4 psia. From Reference 4 it was found that the slope of the vapor-pressure curve for parahydrogen in the neighborhood of the absolute pressure of the hydrogen was

$$m = \frac{dT}{dP} = .41916^{\circ}\text{R/psi}.$$

From Reference 4 it was also found that the temperature of para-hydrogen at 13.54 psia is 36°R . This point is taken as reference, so that the equation for the slope of the vapor-pressure curve in this restricted range can be written as

$$m = \frac{T_R - T_0}{P - P_0}$$

where $m = 0.41916$

$$T_0 = 36^{\circ}\text{R}$$

$$P_0 = 13.54 \text{ psi}$$

Rearranging the equation gives

$$T_R = m(P - P_0) + T_0$$

or

$$T_R = .41916 (P - 13.54) + 36.$$

In this equation, P is the total pressure on the dewar

$$P = P_{\text{atmospheric}} + P_{\text{dewar}}$$

where $P_{\text{atmospheric}} = (\text{barometric-gage reading, or } B \text{ in.-Hg}) \times (\text{constant})$

$$= (B \text{ in.-Hg}) \times (.49116 \text{ psi/in.-Hg})$$

and $P_{\text{dewar}} = (\text{pressure-transducer output, or } P_0 \text{ mv}) \times (\text{calibration factor of transducer})$

$$= (P_0 \text{ mv}) \times (.45475 \text{ psi/mv})$$

Thus the correct temperature of the LH_2 at any particular time is

$$T_R = .41916 (B) \left[(.49116) + (P_0) (.45475) - 13.54 \right] + 36$$

3.4 Discussion

The initial calibration cycle run at ice-bath and LN_2 temperatures indicated that resistance values for several of the RTT's were not as predicted by their calibration curves. It was found that four of the shielded RTT's (S/N's 6320, 6317, 8929, and 6576) had low resistance readings from element to case at room temperature. These four, along with eight others that were apparently good, were sent to AGC for analysis. All but two of the RTT's were returned to NARF for reinstallation. The two that were not returned were S/N's 8929 (hafnium-cadmium shielding) and 6576 (hafnium shielding). Also, S/N 9991 was deleted from the test in order to

add another shielded RTT. S/N 6320 (cadmium shielding) was not reinstalled.

After reinstallation of the RTT's, the ice-bath and LN_2 calibration cycle was again made and data recorded. These data showed that S/N's 6317 and 211 had bad resistance readings for the ice-bath and LN_2 temperature cycles and that S/N 12330, which was one of the replacement RTT's (hafnium-cadmium coating), had a low resistance reading for the ice-bath cycle but a good reading at LN_2 temperatures. The decision was made to continue with the test. The subsequent preirradiation LN_2 cycles failed to show any problems with any of the RTT's.

The irradiation began at 23:54 on 22 June with an initial step to 1 Mw. The 1-Mw step was held for approximately 30 min and was followed by a step to 2-Mw for approximately 30 min. The reactor power was then increased to 3 Mw, and a routine data schedule of three data cycles per hour was initiated. When inspection of the data taken at 3 Mw revealed that periodic interruptions of the irradiation would be required to obtain zero dose-rate readings, 6-hr intervals (changed to 4-hr intervals half way through the test) were scheduled. The interruptions were accomplished by retracting the GTR from the closet for the period of time required to obtain a data cycle.

A problem with liquid-hydrogen supply was encountered early in the test. Since the initial LH₂ trailer had experienced a great deal of boil-off before the test started, a routine trailer change was made on 23 June. When it became apparent that the use rate from the second trailer was higher than expected, an attempt was made to expedite the schedule of another LH₂ trailer; but no trailers could be scheduled to the Fort Worth Division in time to prevent loss of cryogen at the use rate being experienced with the reactor at power. A meeting of AEC and Fort Worth Division personnel was then held, and the decision was made to shut down the reactor in order to minimize the use rate and thereby maintain the RTT's in LH₂ until a replacement trailer arrived. Because transportation involved factors beyond local control, the replacement trailer did not arrive until 3 hr after the trailer in use was depleted. Data was taken during the 3-hr warm-up. When the replacement trailer was installed and liquid hydrogen reintroduced, a calibration data cycle of the RTT's was obtained and the irradiation was resumed at approximately 2400 hours on 25 June.

After resumption of the irradiation, the test proceeded routinely until 30 June. On that date, a routine LH₂ trailer change resulted in the LH₂ level dropping below the RTT's for a period of 1 min. This drop was due to a leak in the vacuum jacket of a LH₂ transfer line.

On 1 July - 34 hr before the scheduled completion of the test - problems began to occur with the GTR traversing mechanism during the scheduled retractions. The possibility that the mechanism might fail with the GTR retracted could not be discounted and the remaining scheduled retractions were cancelled.

Upon completion of the 600 Mr-hr of irradiation, the reactor was retracted and shut down. The LH_2 level was maintained for 2 hr after reactor shutdown. During this time, data were taken at the rate of 1 cycle every 5 min for the first hour and 1 cycle every 10 min for the second hour. Then the LH_2 supply was shut off. After the liquid in the dewar had been depleted, warm-up was initiated by passing hot GN_2 through the dewar. During the warm-up, data were taken 1 cycle every 15 min. Maximum temperature inside the dewar was approximately 90°C .

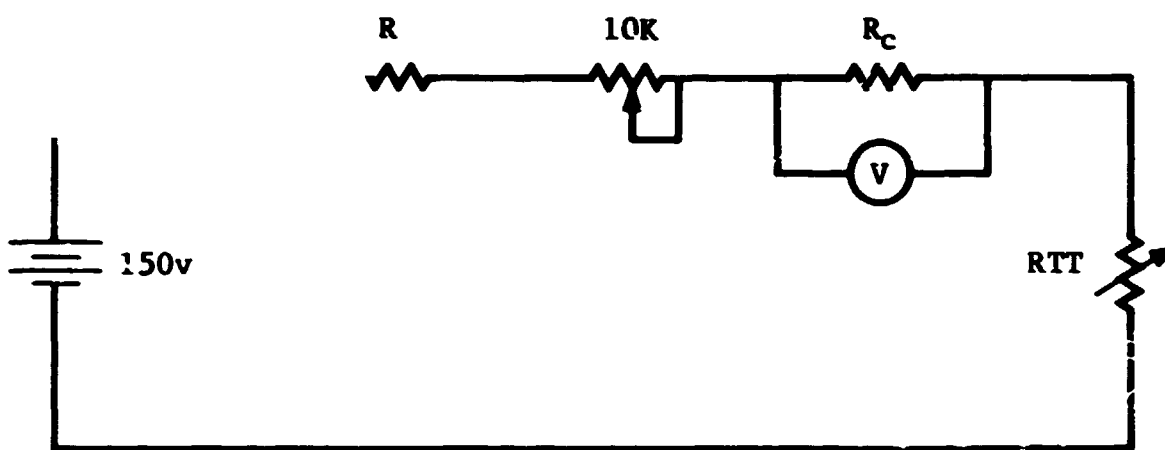


Figure 3-1 RTT Calibration Circuit

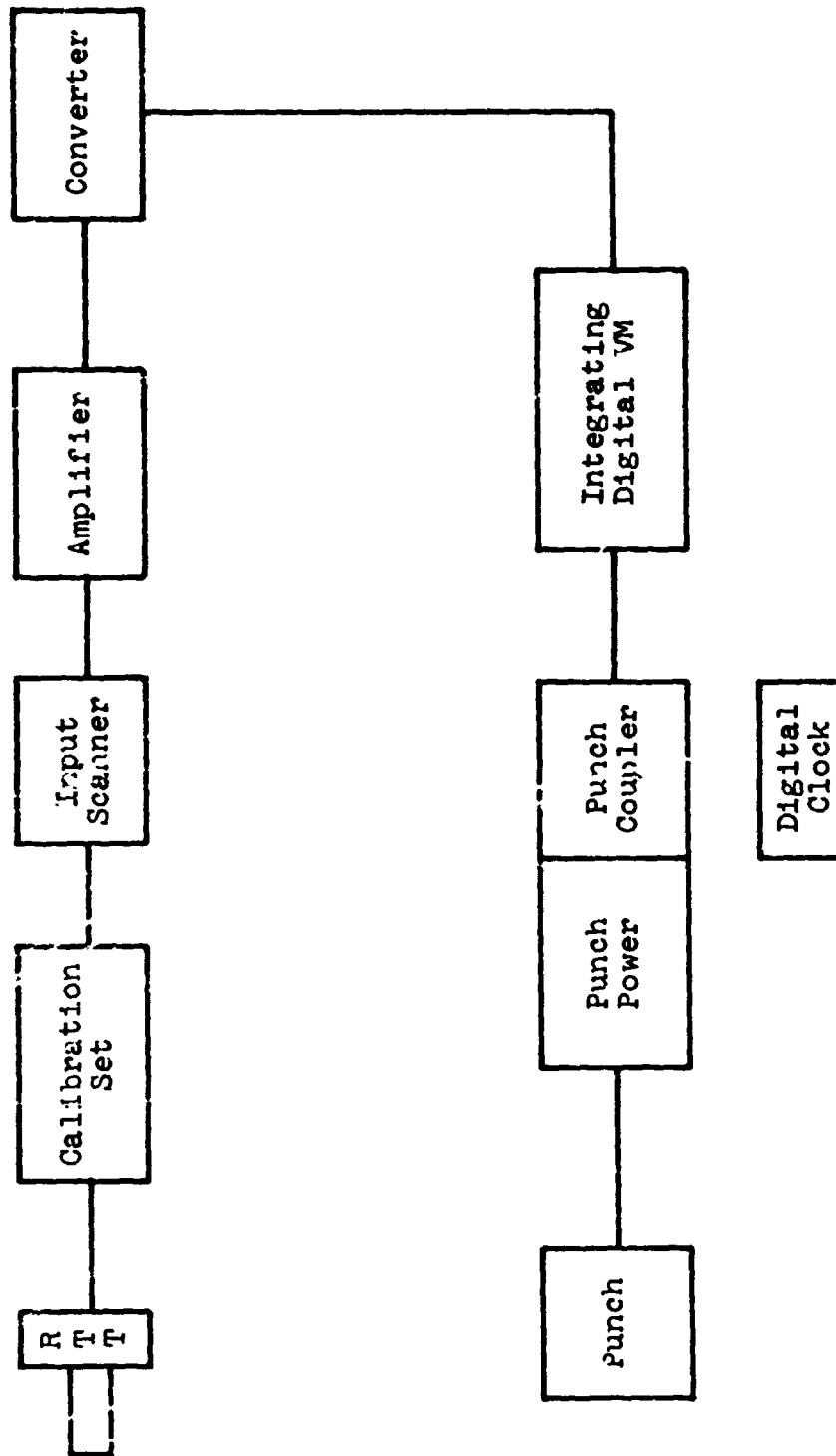


Figure 3-2 Block Diagram for RTT Test

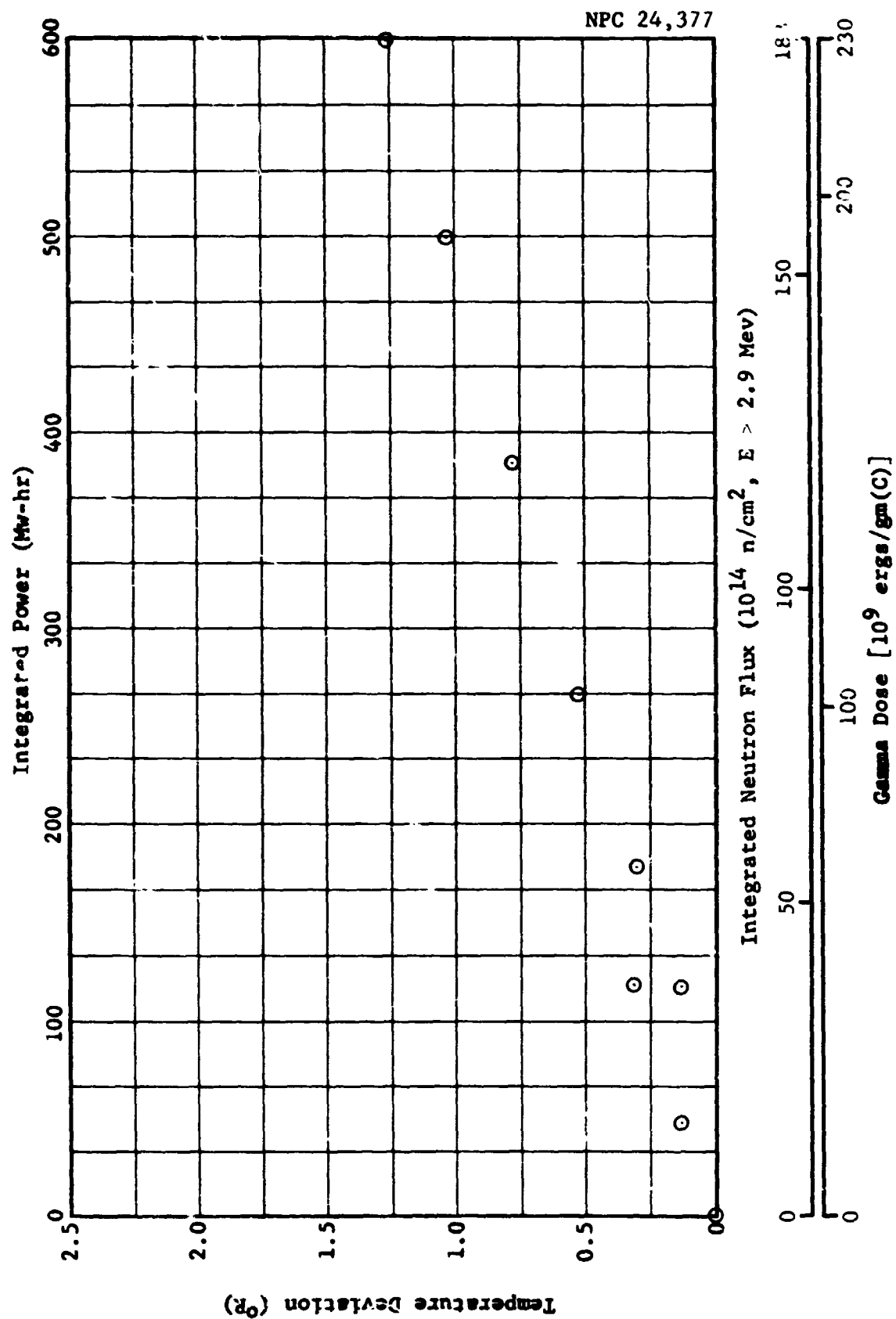


Figure 3-3 Temperature Deviation vs Radiation Exposure:
RTT 1 (Rosemount 134EB186, S/N 8927), Cadmium Shielded

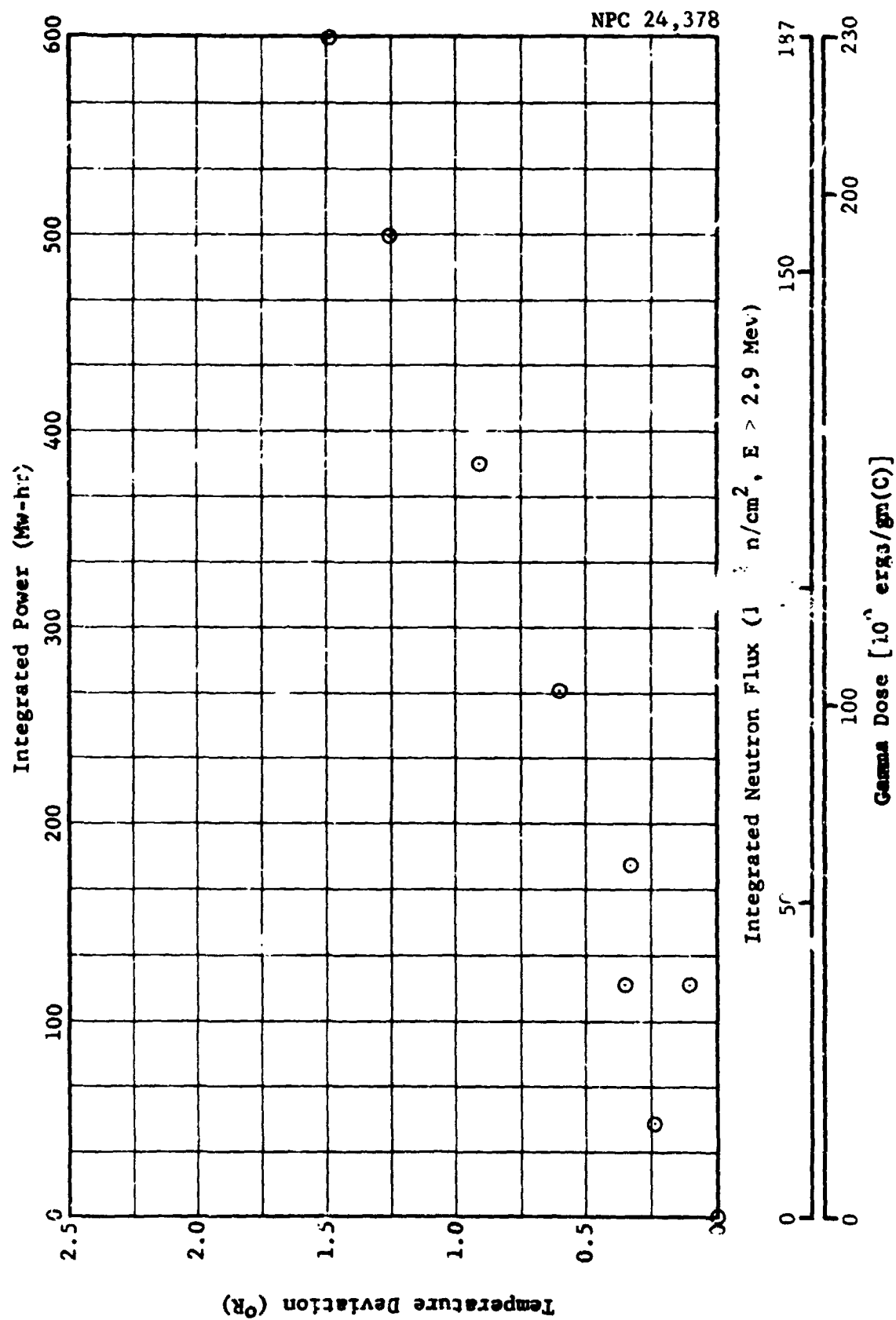


Figure 3-4 Temperature Deviation vs Radiation Exposure:
RTT 2 (Rosemount 134EB186, S/N 12313), Cadmium Shielded

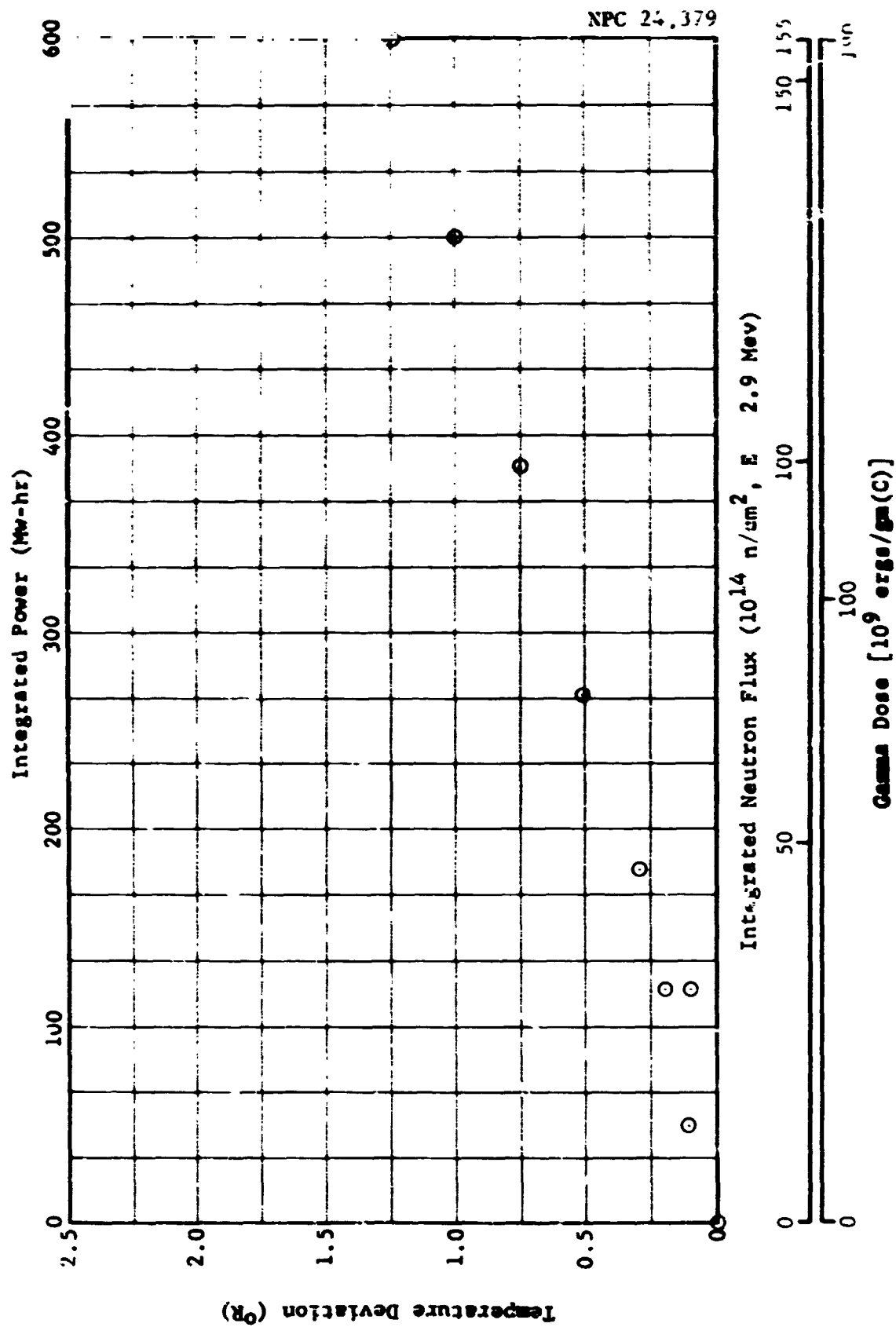
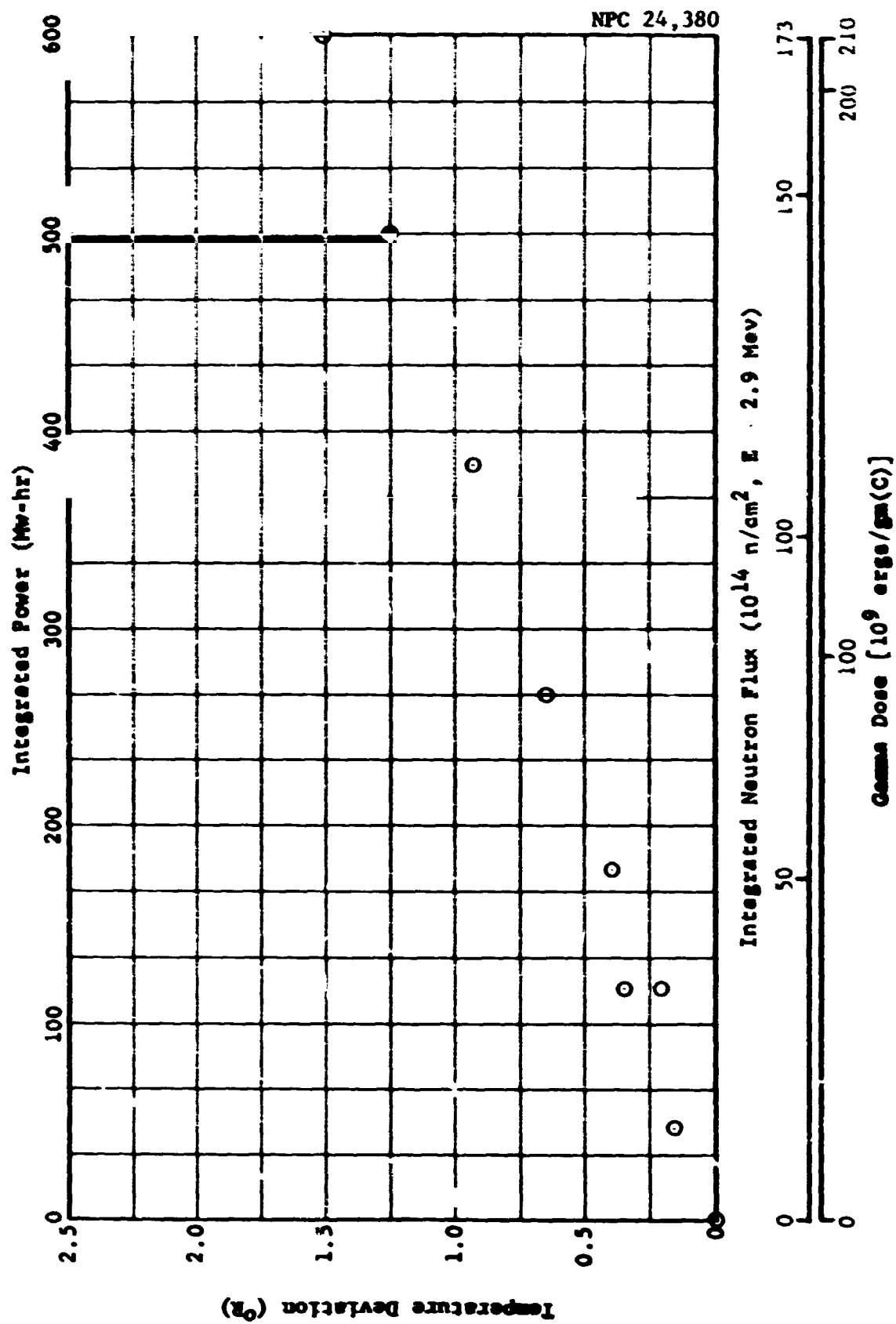


Figure 3-5 Temperature Deviation vs Radiation Exposure;
 RFT 3 (Rosemount 134EB186, S/N 6317), Hafnium-Cadmium shielded



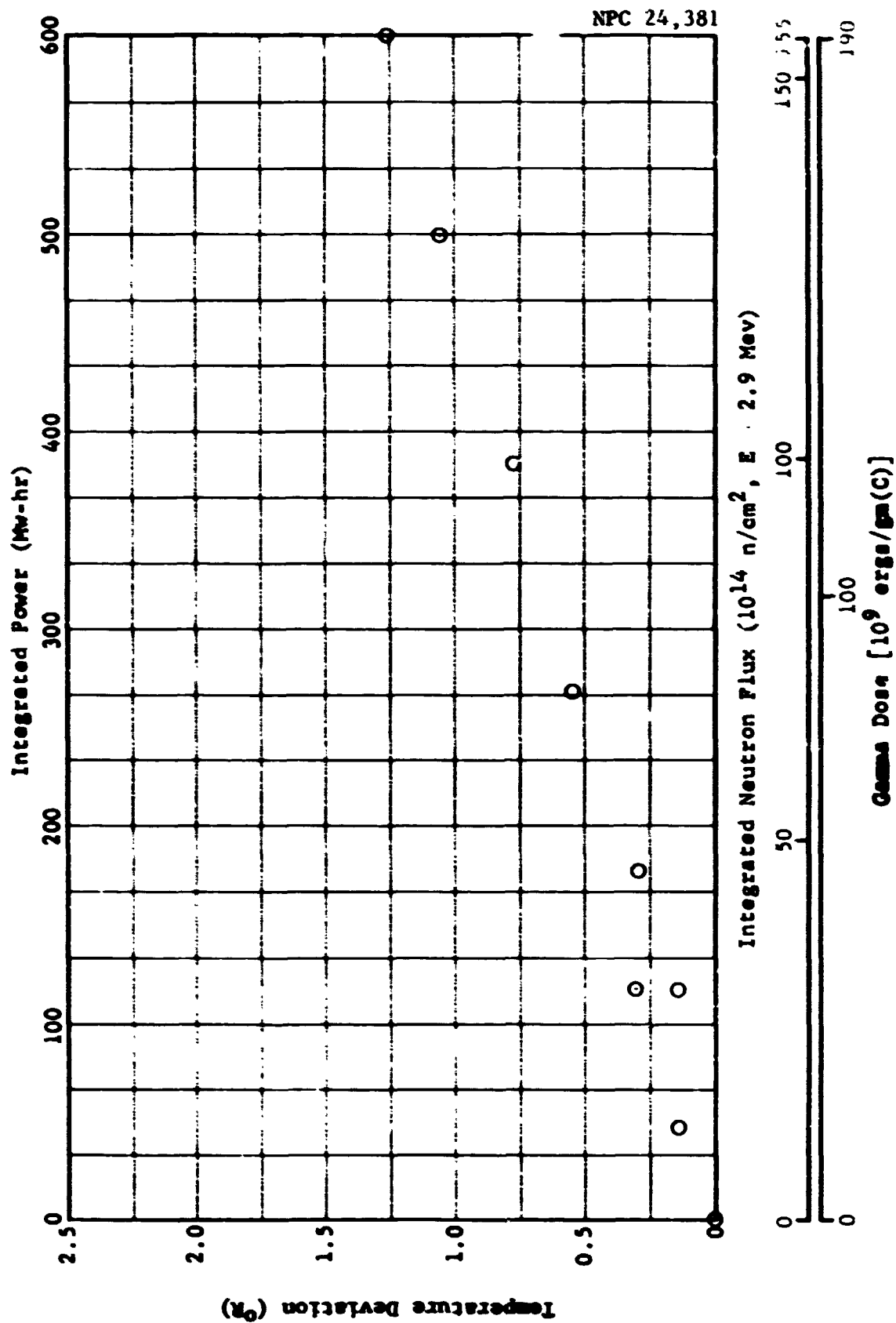


Figure 3-7 Temperature Deviation vs Radiation Exposure:
RTT 5 (Rosemount 134EB186, S/N 4092), Hafnium Shielded

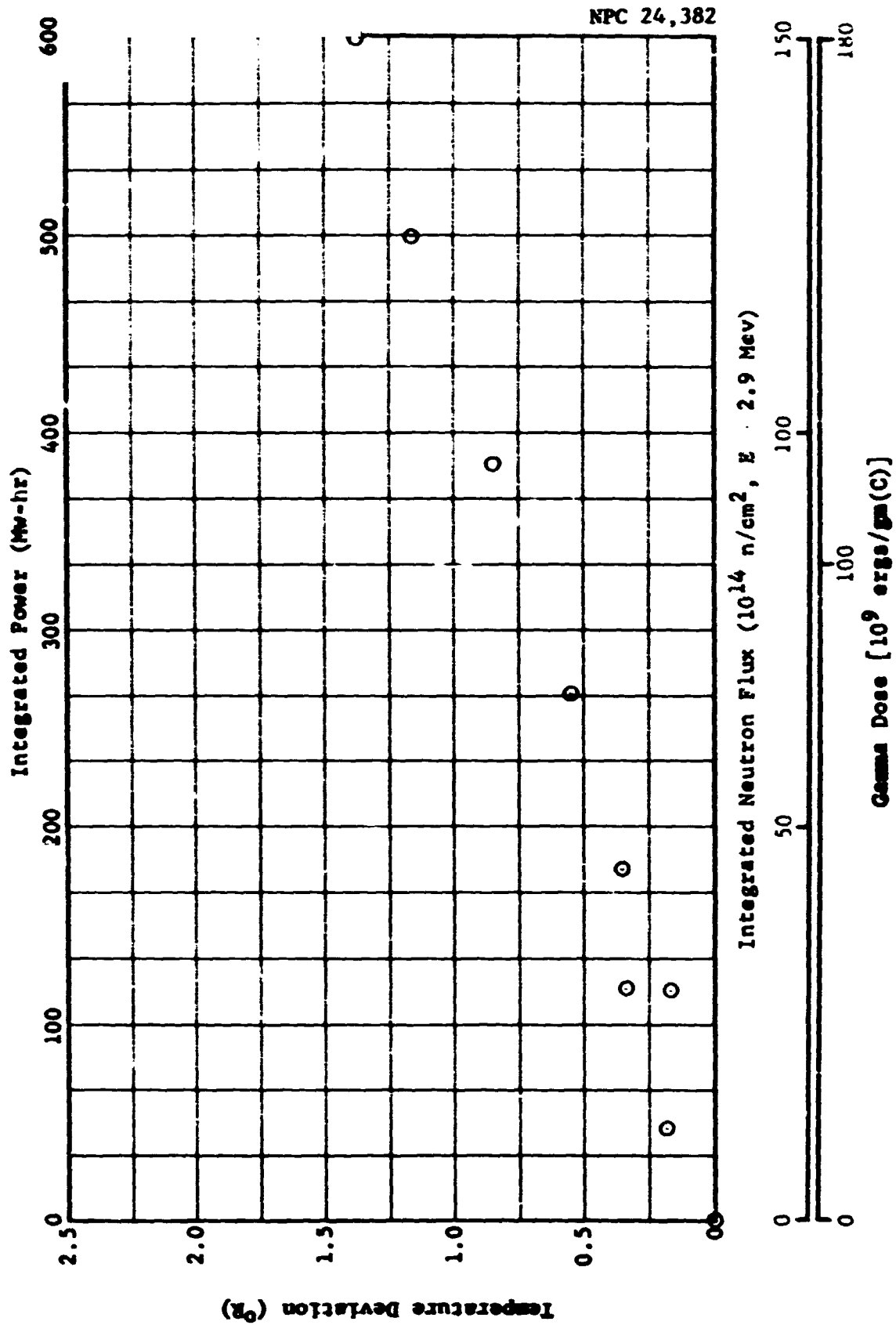


Figure 3-8 Temperature Deviation vs Radiation Exposure:
RTT 6 (Rosemount 134EN186, S/N 12340), Hafnium Shielded

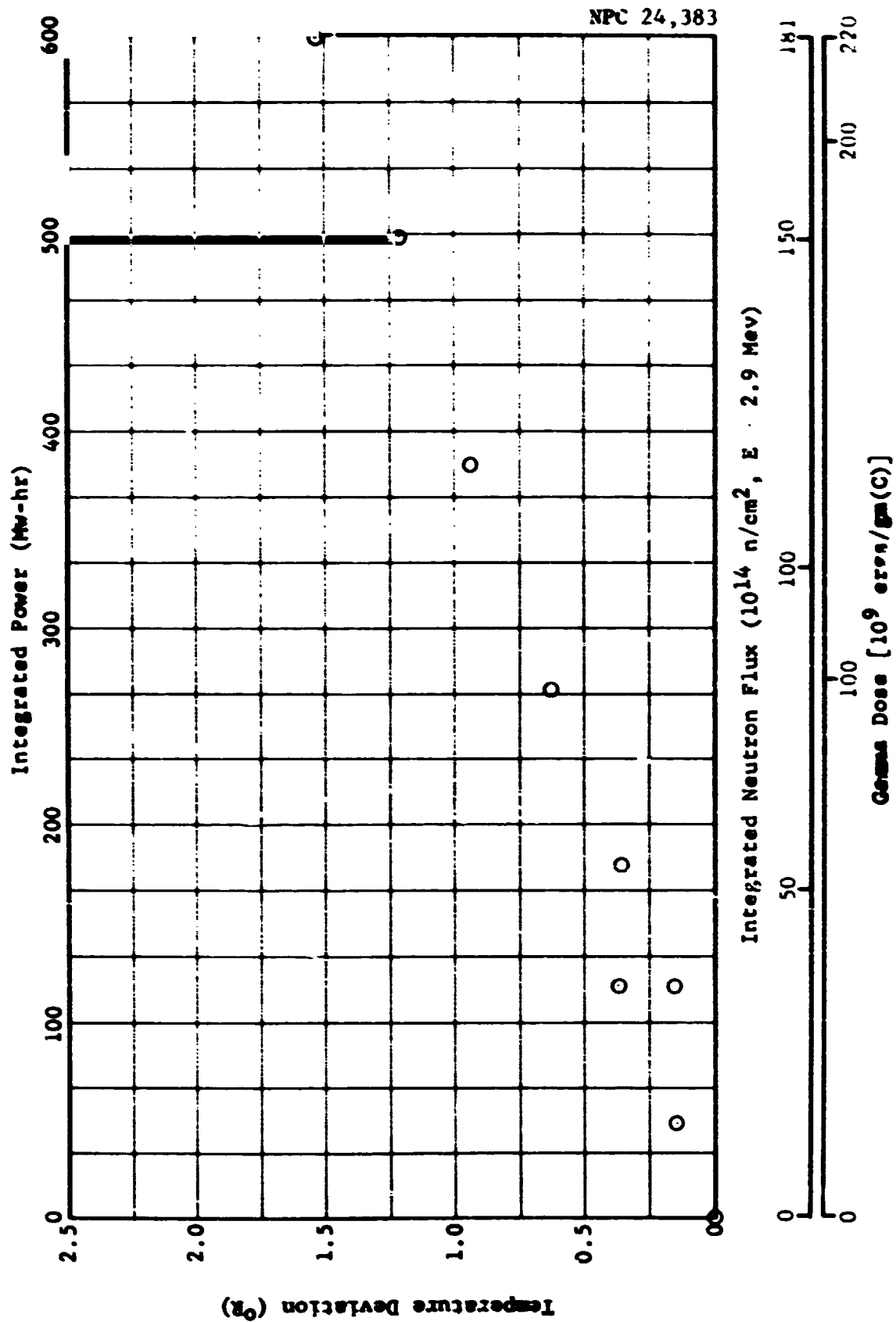


Figure 3-9 Temperature Deviation vs Radiation Exposure:
RTT 7 (Rosemount 134EB186, S/N 4094)

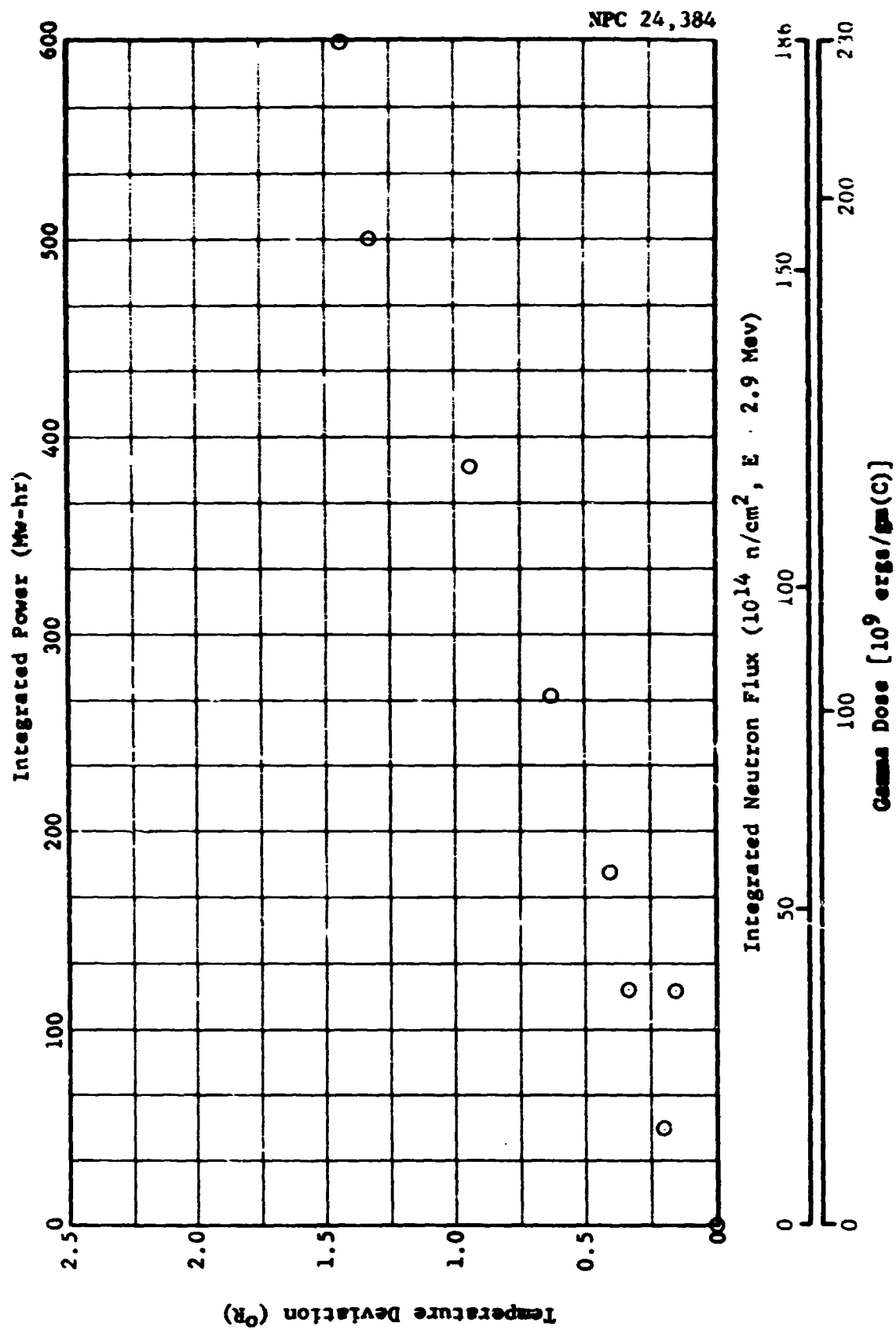


Figure 3-10 Temperature Deviation vs Radiation Exposure:
RTT 8 (Rosemount 134EB18C, S/N 4096), Stainless-Steel Shielded

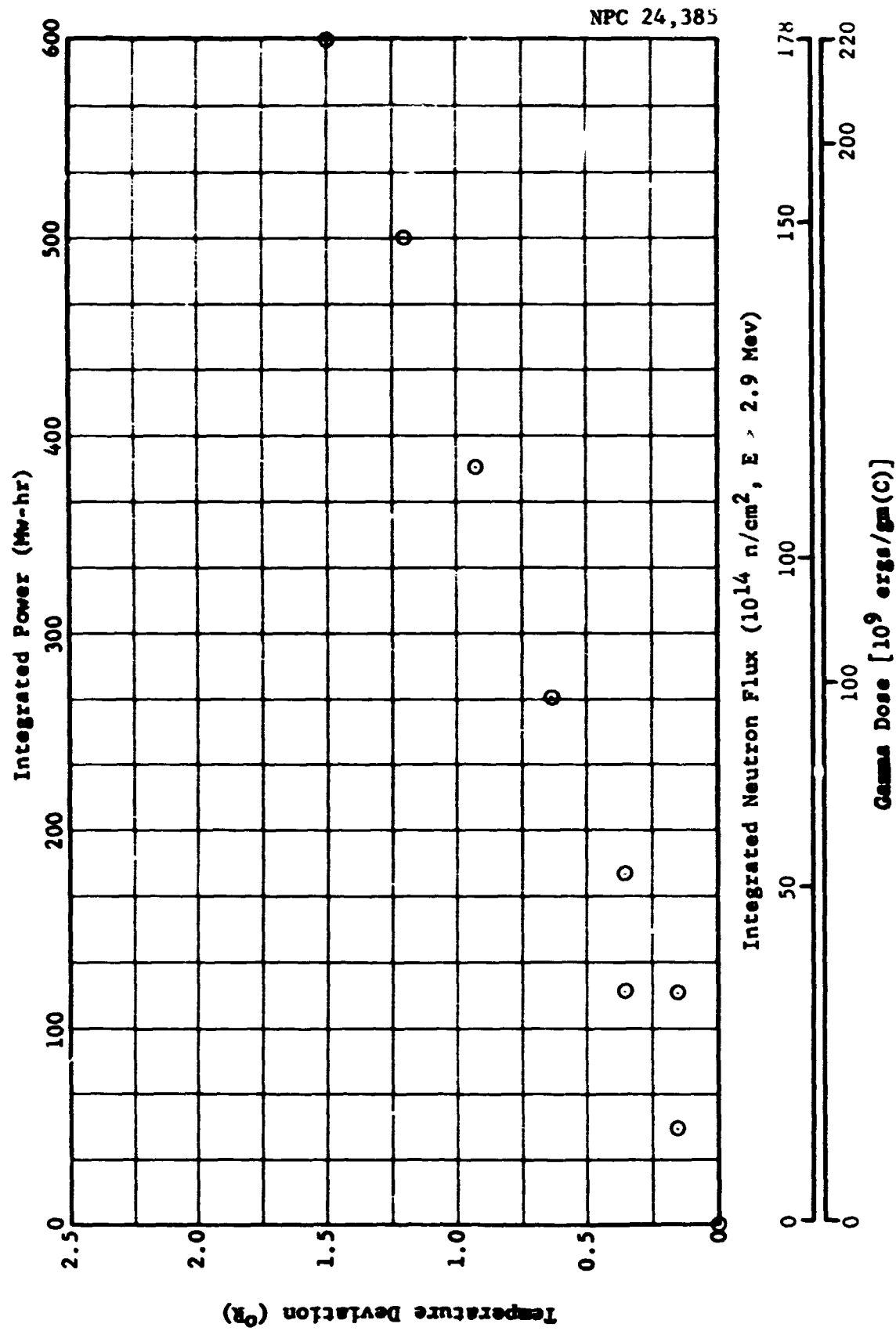
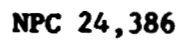


Figure 3-11 Temperature Deviation vs Radiation Exposure:
RTT 9 (Rosemount 134EB186, S/N 4104)



**Figure 3-12 Temperature Deviation vs Radiation Exposure:
RTT 10 (Rosemount 134EB186, S/N 6319), Stainless-Steel Shielded**

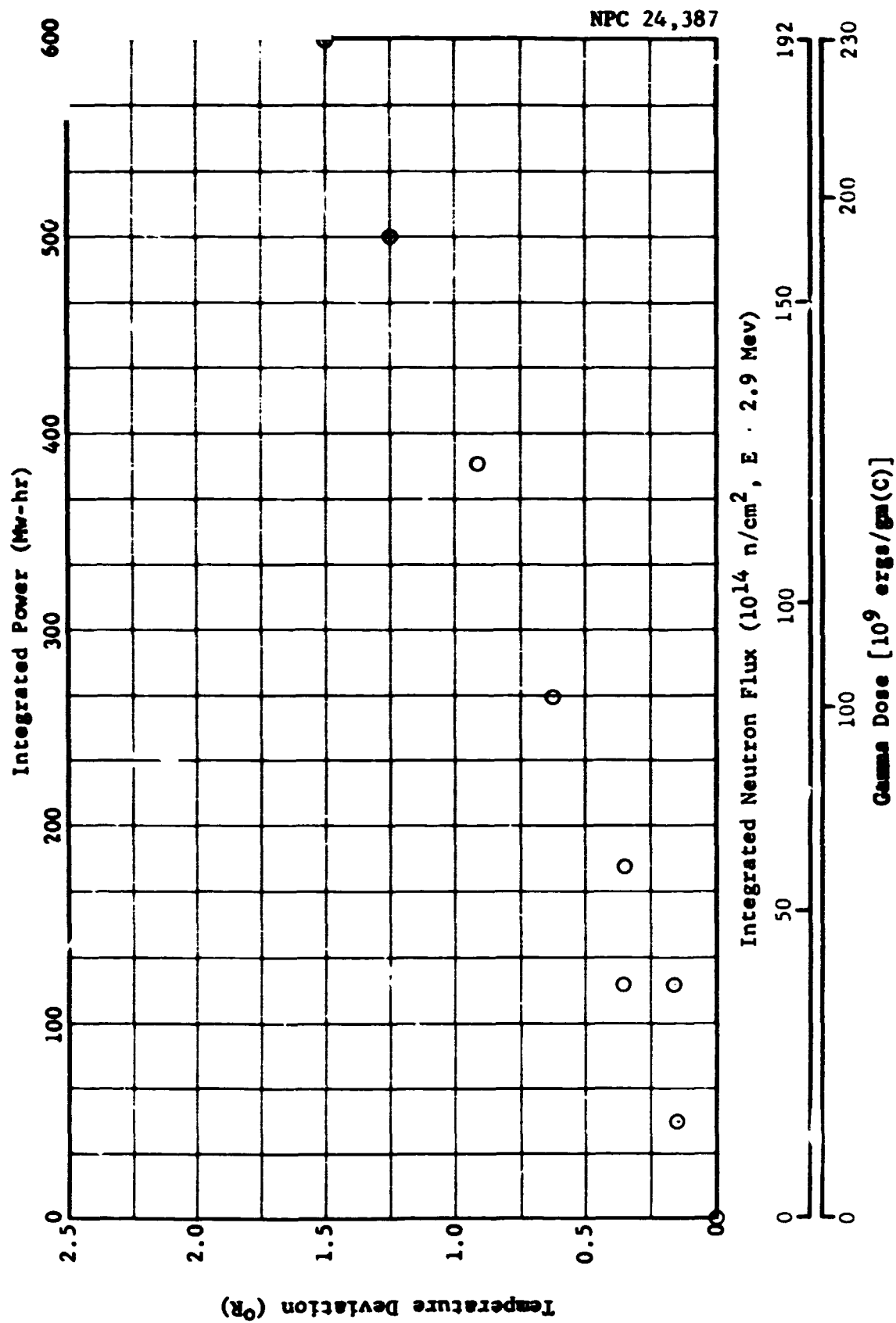


Figure 3-13 Temperature Deviation vs Radiation Exposure:
RTT 11 (Rosemount 134EB186, S/N 7365), Hafnium-Cadmium Shielded

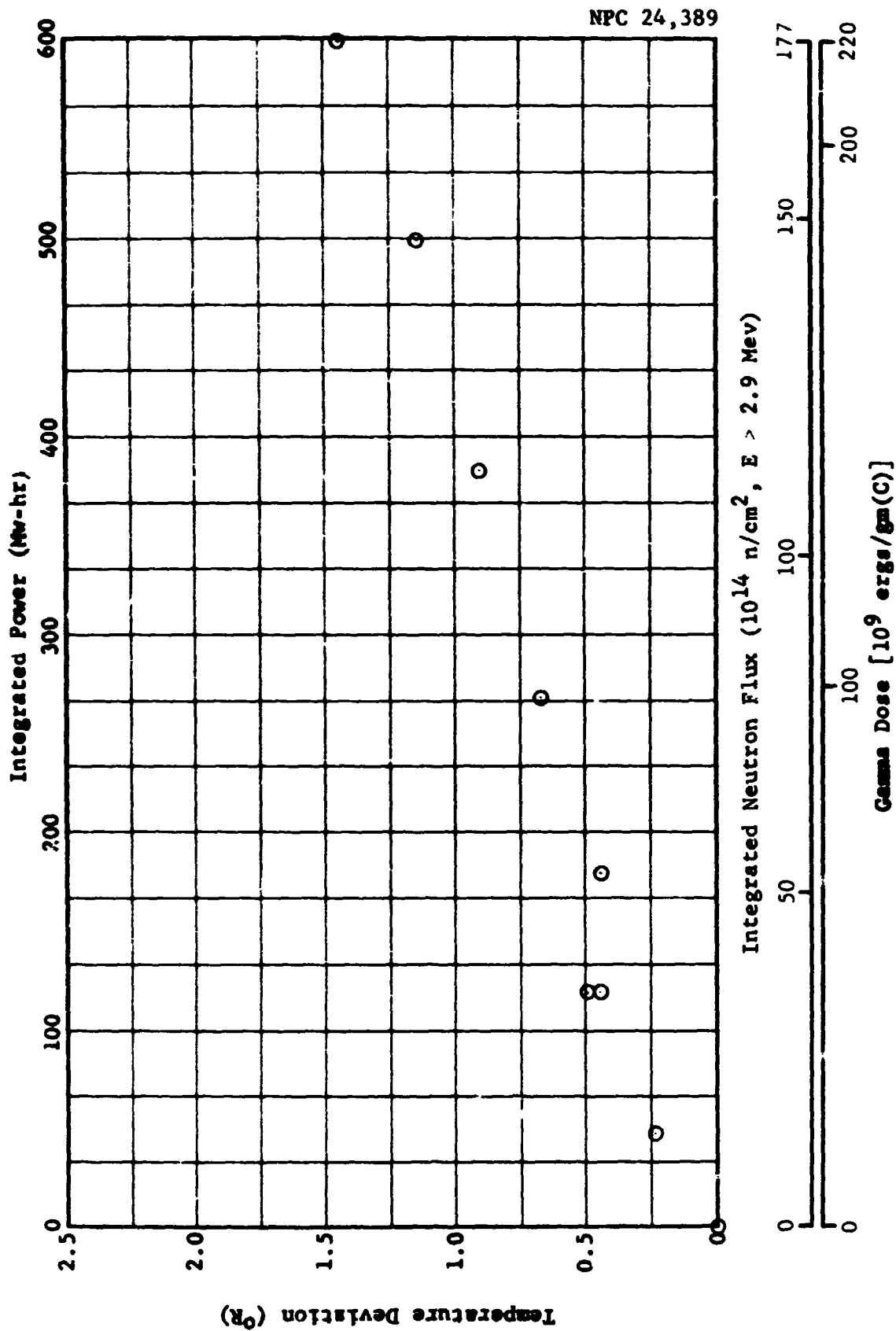


Figure 3-15 Temperature Deviation vs Radiation Exposure:
RTT 13 (Rosemount 134EB2X, S/N 9371)

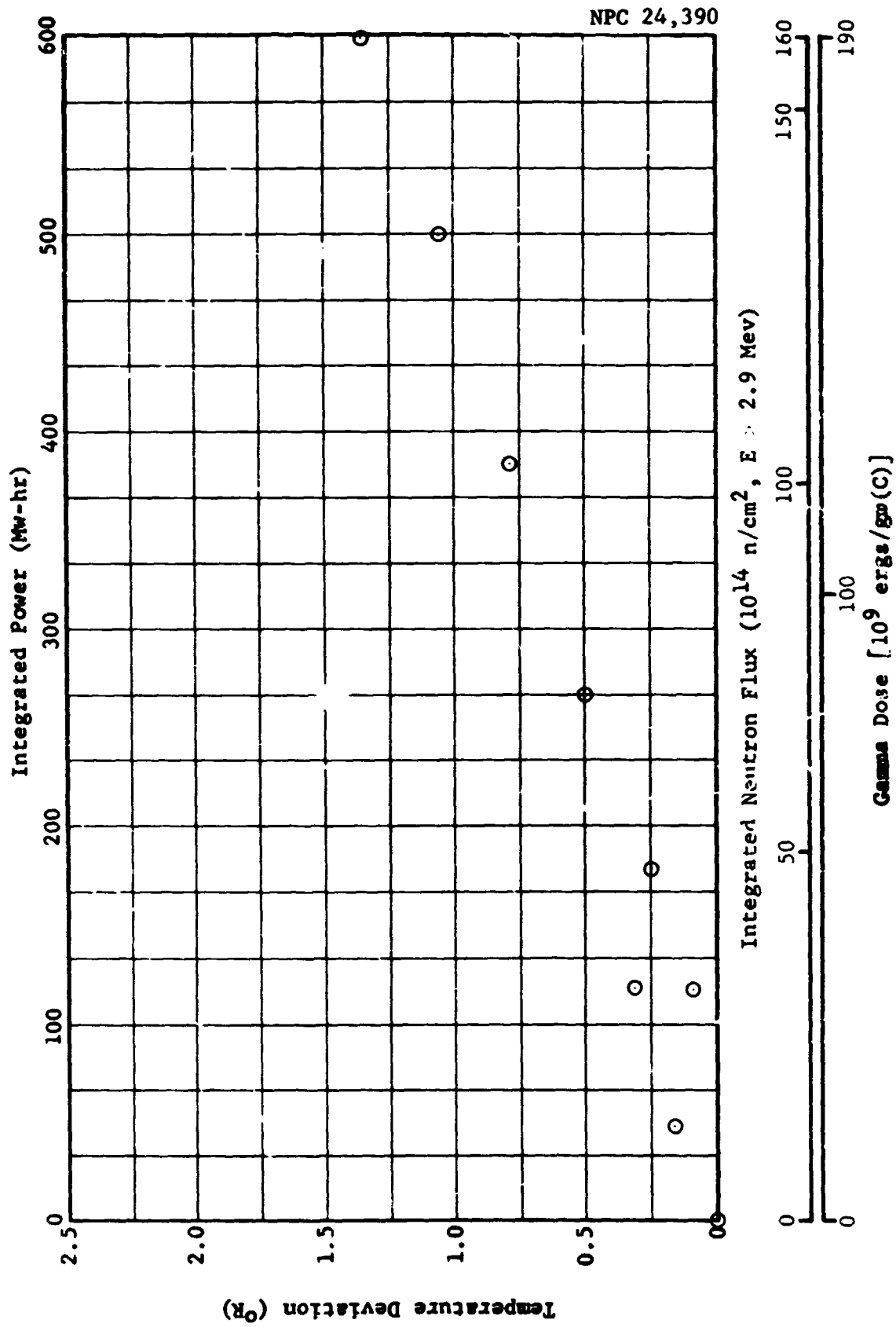


Figure 3-16 Temperature Deviation vs Radiation Exposure:
RTT 14 (Rosemount 134EB2X, S/N 9370)

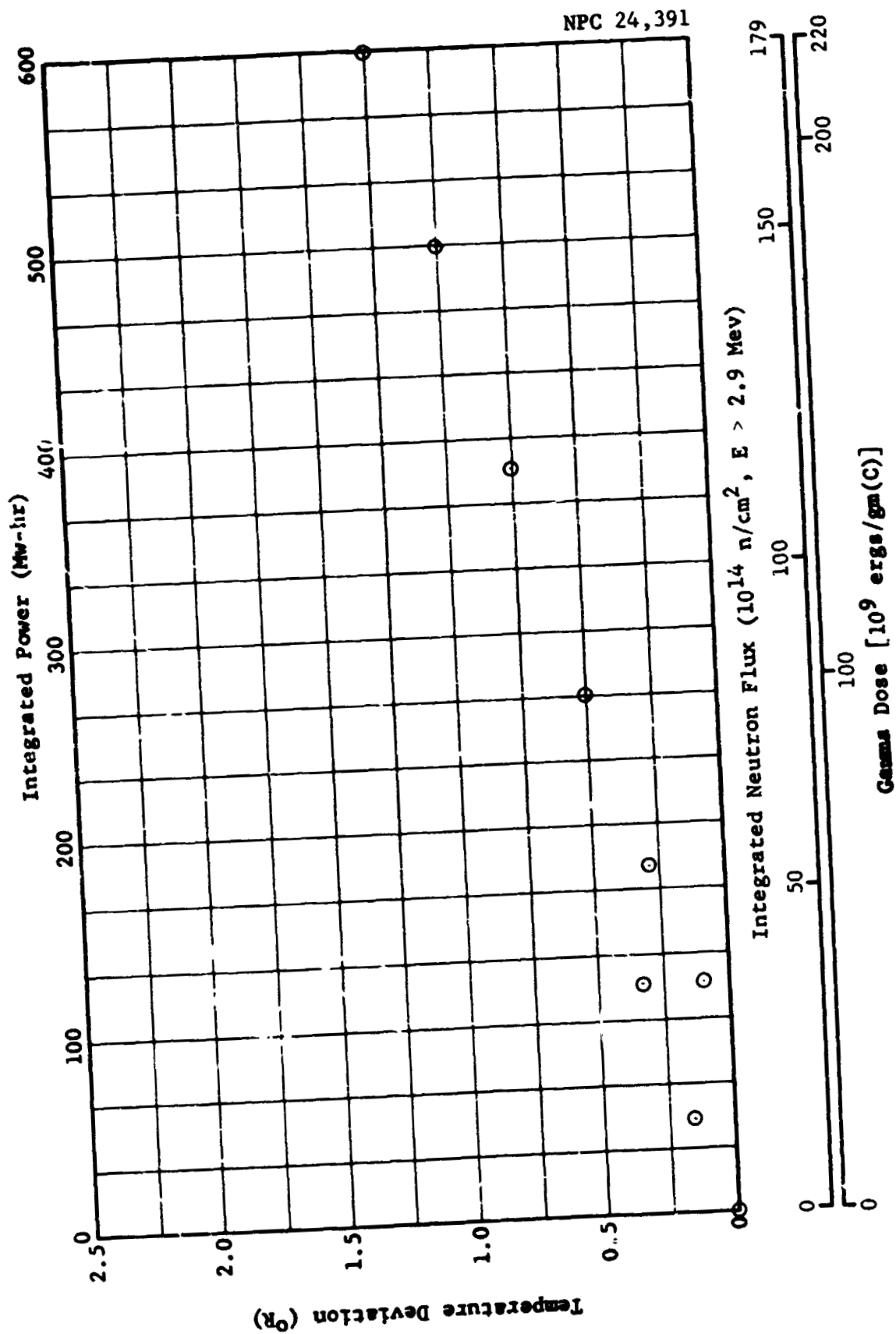


Figure 3-17 Temperature Deviation vs Radiation Exposure:
RTT 15 (Rosemount 137CJ, S/N 1667)

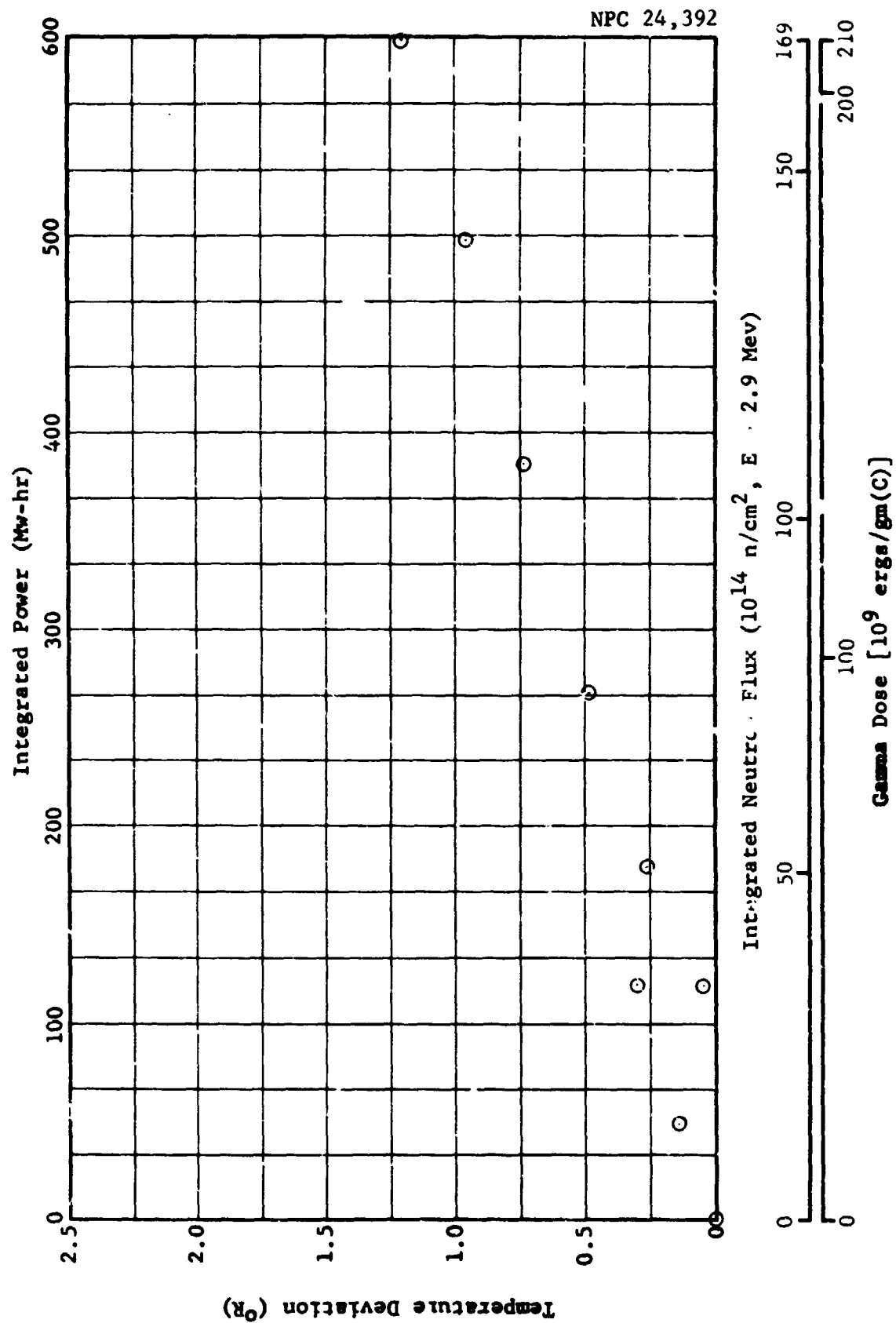


Figure 3-18 Temperature Deviation vs Radiation Exposure:
RTT 16 (Rosemount 137CJ, S/N 1666)

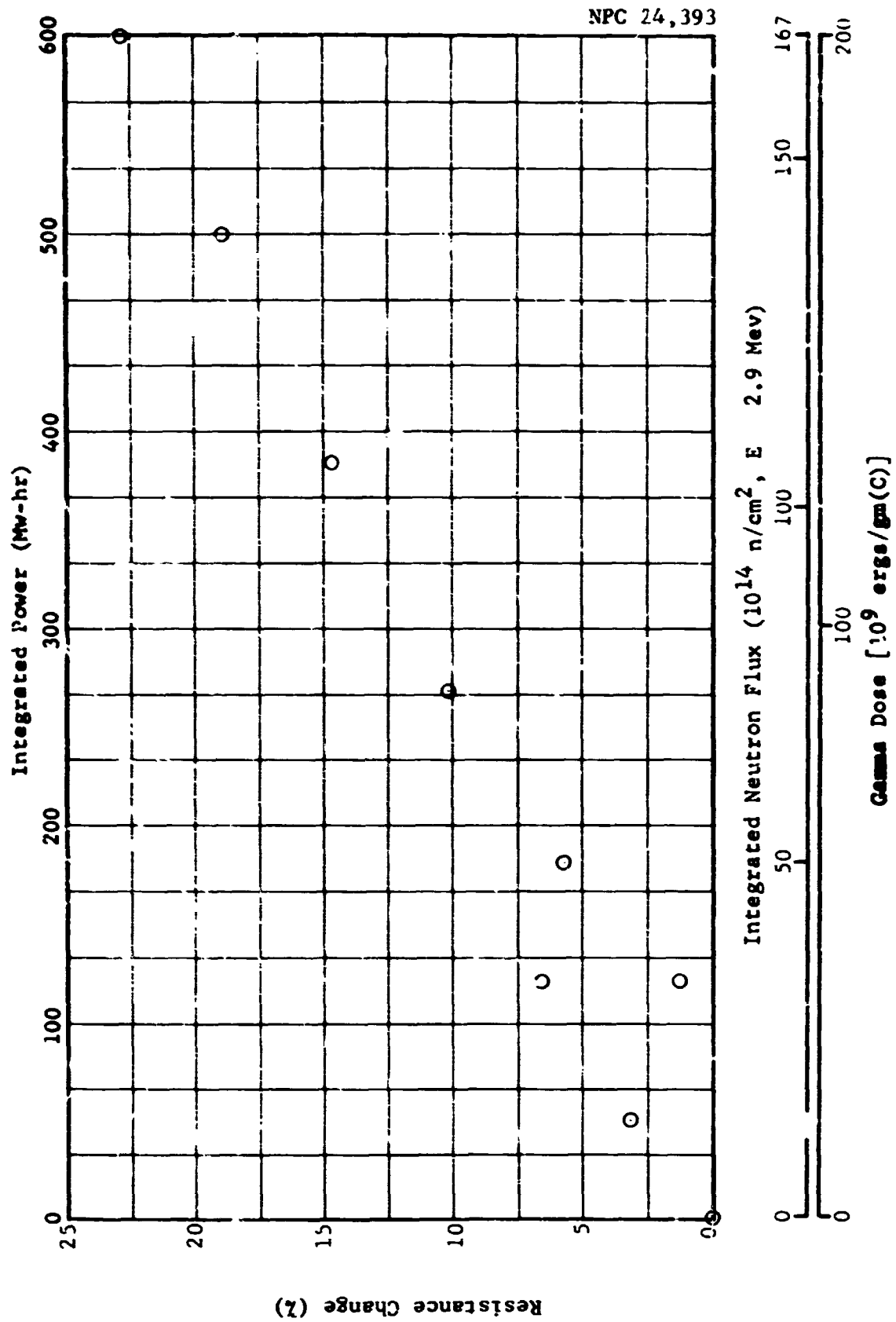


Figure 3-19 Percent Resistance Change vs Radiation Exposure:
RTT 17 (Temtech 1881-2, S/N 6149)

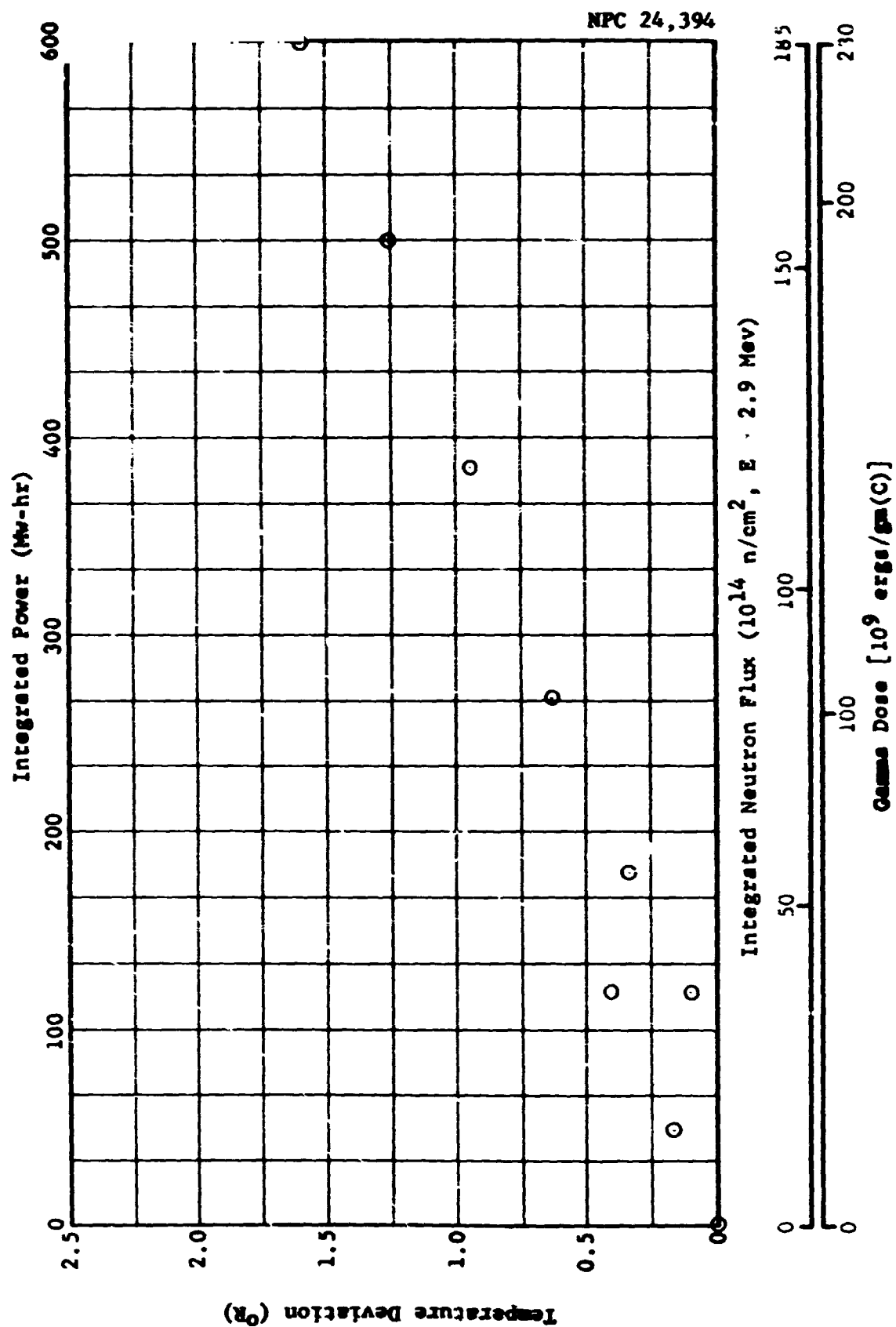


Figure 3-20 Temperature Deviation vs Radiation Exposure
RTT 18 (Rosemount 134EB250, S/N 4107)

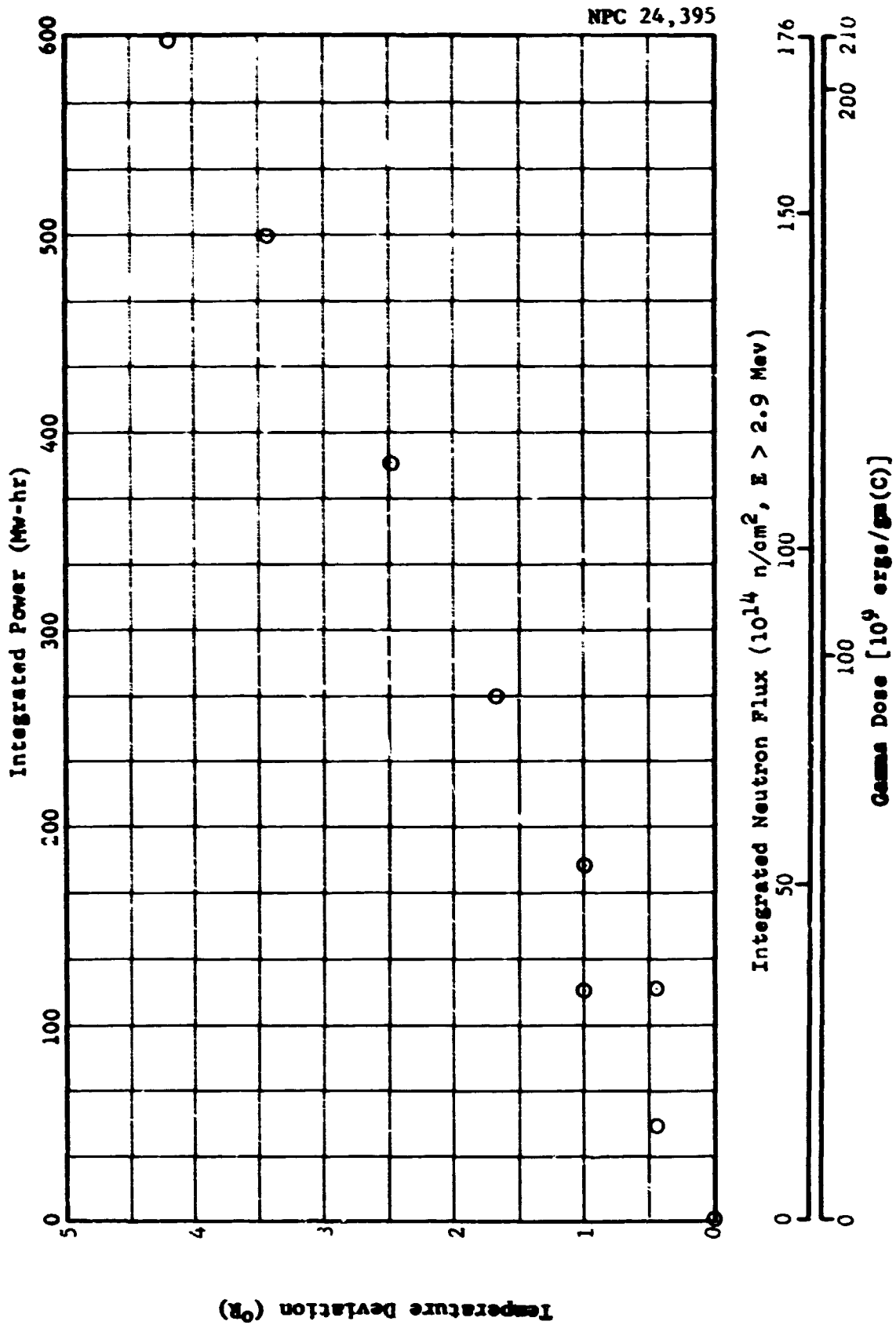


Figure 3-21 Temperature Deviation vs Radiation Exposure:
RTT 19 (Rosemount 110AA, S/N 211)

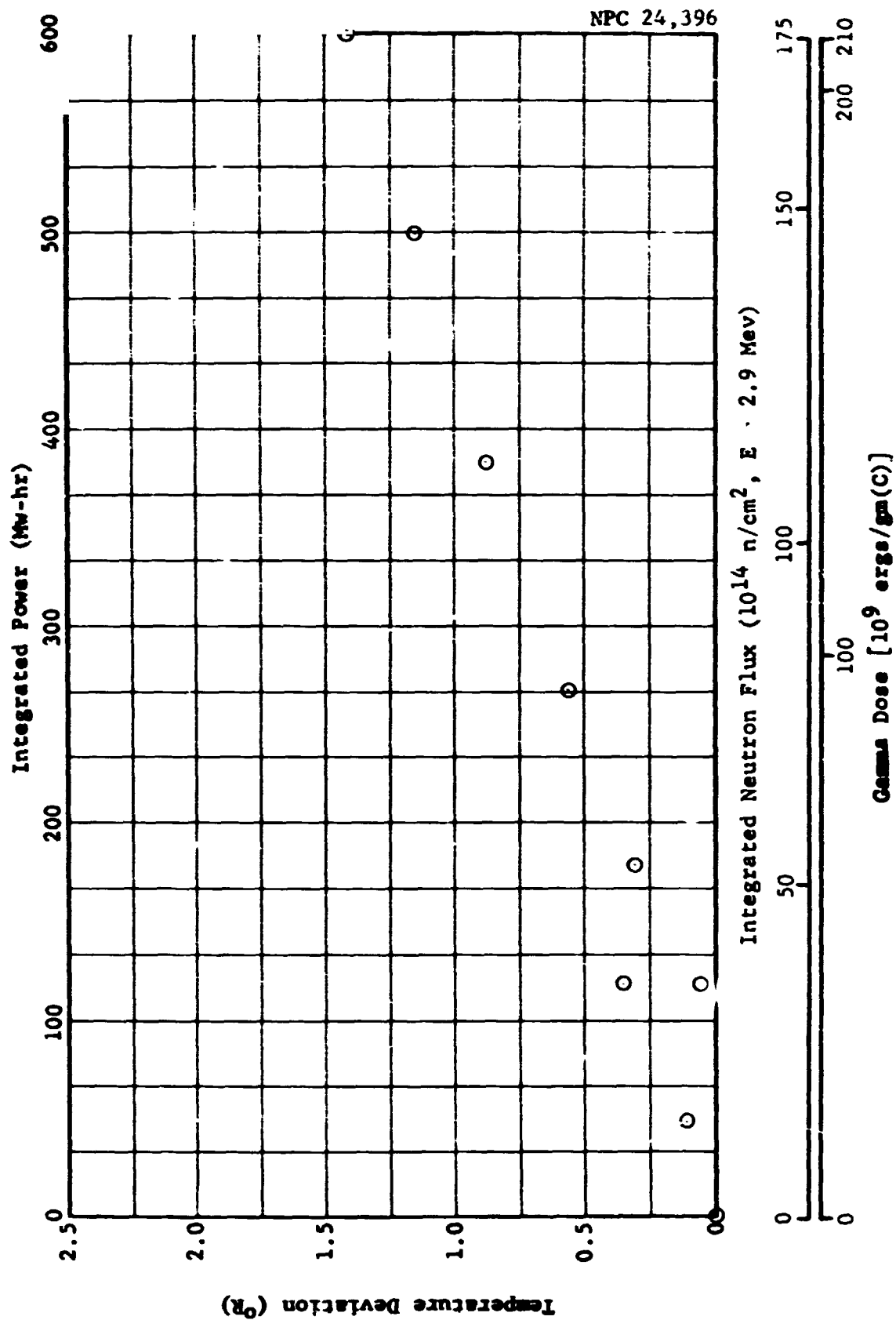


Figure 3-22 Temperature Deviation vs Radiation Exposure:
RTT 20 (Rosemount 134EB1X, S/N 9373)

BLANK PAGE

IV. PARAHYDROGEN-ORTHOHYDROGEN CONVERSION

4.1 Purpose

A measurement of the para-ortho composition of effluent hydrogen gas from the liquid-hydrogen irradiation portion (RTT test) of GTR 18 was undertaken. The purpose of this effort was to attempt to detect radiation-induced composition changes and thereby gain some insight into the effects of reactor radiations on liquid and/or gaseous hydrogen.

The measurement was made with an Apogee Development Corporation Apogee General Purpose Gas Analysis System (AGPGAS), loaned to General Dynamics for this purpose by the National Bureau of Standards (NBS).

4.2 Discussion

The hydrogen atom, simplest of all the elements, is composed of a nucleus, consisting of one proton, and one orbiting electron. Both the nucleus and the electron are free to spin in either direction; hence, four configurations of the atom are possible. However, to form the diatomic molecule, only those atoms having opposite electron spin are free to combine. Thus, the four atomic configurations can combine in such a way as to produce only two molecular configurations: one in which the spins of the two nuclei are parallel, called orthohydrogen and one in which the spins are anti-parallel, called parahydrogen.

The nuclear spins of the molecules contribute to the total rotational energy of the molecule, which exists at discrete levels denoted by the rotational quantum number J . Either modification (orthohydrogen or parahydrogen) can exist in a number of different excited states corresponding to increasing values of J ; but the para modification is restricted to the even rotational quantum numbers, and the ortho modification is confined to the odd quantum numbers. At temperatures below about 80°K , almost all molecules are in the ground state, i.e., the energy levels represented by $J=0$ for parahydrogen and $J=1$ for orthohydrogen. Between these two lowest levels, the energy gap is about 339 cal/mole (about 0.015 ev/molecule).

A definite equilibrium ratio, β , between the ortho and para fractions of hydrogen gas exists for any given gas temperature. Farkas (Ref. 7) gives the following expression for

$$\beta = \frac{P - H_2}{O - H_2} = \frac{\sum_{J = \text{even}} (2J + 1)e^{-J(J + 1)B/KT}}{\sum_{J = \text{odd}} 3(2J + 1)e^{-J(J + 1)B/KT}} \quad (1)$$

where J = rotational energy level = 0, 1, 2, 3, ...

$$B = \frac{\hbar^2}{2I}$$

\hbar = Planck constant $\div 2\pi$

I = moment of inertia of the molecule

K = Boltzmann constant

T = absolute temperature

From Equation 1, it can be seen that at higher temperatures β approaches the limiting ratio 1:3. This also is essentially the ratio obtained at room temperature; hence, the term "normal hydrogen" has come to be used to describe hydrogen composed of 25% parahydrogen and 75% orthohydrogen. Correspondingly, the term "equilibrium hydrogen" is used to specify hydrogen in which the two modifications are in equilibrium at some temperature, usually other than room temperature.

In general, the equilibrium conditions described by Equation 1 are not obtained without catalysis, because of the very slow reaction rates involved. For instance, ortho-para conversion by radiation emission has been estimated at about one transition in 300 years, and transition by collision has been estimated as having a half-life of three years (Ref. 7). Parahydrogen, free from contaminants, is a very stable gas and can be stored for weeks at room temperature without conversion. Although the molecules will be excited above the ground state (in conformance with Equation 1), only the even quantum levels will be populated.

There are two basic methods by which ortho-para transitions may be induced:

1. Forcing dissociation of the molecule so that the freed atoms can recombine.

2. Causing the hydrogen molecule to come into sufficiently close proximity to the magnetic field of a paramagnetic substance so as to suffer a spin reversal of one of the protons. A spin reversal of either proton is tantamount to conversion.

Both methods are of interest to this test because either can be an effect of exposure to ionizing radiation.

The energy deposited in liquid hydrogen by nuclear radiation is initially transferred to scattered electrons in the case of gamma radiation and recoil protons in the case of neutron radiation. As these charged particles pass through the liquid, approximately equal amounts of energy go into the production of H atom pairs and H_2 ions, which in turn cause further disassociation, ionization, and excitation. Carter estimates that about 43% of the deposited energy is temporarily stored in the production of such species, the remainder being given up almost immediately as heat (Ref. 3).

Because conversion from parahydrogen to orthohydrogen can have a deleterious effect on the performance of a nuclear rocket of the NERVA type, it becomes of importance to investigate the degree of conversion that occurs when liquid hydrogen is exposed to radiation from a nuclear reactor.

4.3 Experimental Setup

4.3.1 Gas Analyzer

The AGPGAS (Fig. 4-1) operates by comparing the thermal conductivity of a sample stream of hydrogen gas with that of a stream of hydrogen

gas having a known parahydrogen concentration. This is accomplished by comparing the resistance of four gas-stream-exposed filaments connected as the four arms of a Wheatstone bridge. The filament temperatures and, therefore, the resistances are related to the thermal conductivities of the gasses passing over them. An exactly linear relationship has been shown to exist between parahydrogen concentration and thermal conductivity of hydrogen; therefore, a measurement of filament resistance constitutes a measurement of parahydrogen concentration. The method is originally due to Farkas (Ref. 7). The AGPGAS itself is modeled after a refinement developed at NBS, described in References 9 and 10.

4.3.2 Sample System

Sample gas for analysis was obtained from the effluent of the AGC dewar used for the RTT test. Orthohydrogen concentration of the dewar supply was 3%.

A secondary loop of $\frac{1}{2}$ -in. copper tubing was tapped into the stationary dewar exhaust system at a point 40 ft downstream from the dewar, routed into and out of the reactor control room via the water-filled access window, and returned to the stationary exhaust system 40 ft downstream of the take-off point. A tertiary loop of $\frac{1}{8}$ -in. copper tubing was used to extract from the secondary loop the small quantity needed to supply the analyzer. The purpose of the system was to deliver irradiated hydrogen to the analyzer in as short a time as possible after it was exhausted from

the dewar. A schematic showing details of the system is shown in Figure 4.2

At equilibrium, LH_2 use rate (at 3-Mw reactor power) averaged 94 gal/hr. Liquid capacity of the dewar is about 30 gal, controlled to plus or minus 1 gal, and ullage is also about 30 gal. On the average, then, the hydrogen had an irradiation history of 19 min as a liquid and 22 sec as a gas.

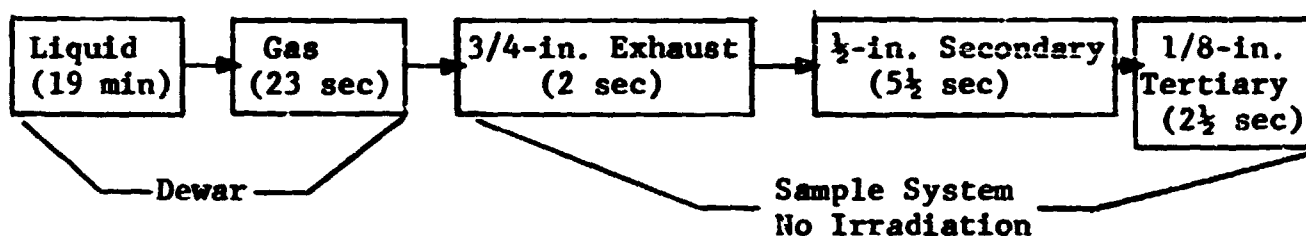
Between the secondary-loop take-off point and the dewar, the exhaust line is 3/4-in. ID flexible stainless-steel pipe. At a use rate of 94 liquid gallons per hour the maximum residence of the effluent is 2 sec in the portion of the pipe between the dewar and the secondary take-off point.

After entering the secondary, the gas traverses 60 ft of 1/2-in. OD copper tubing before entering the tertiary loop. Minimum residence time in this part of the system is calculated as 5 1/2 sec.

After entering the tertiary loop of 1/8-in. copper tubing, the effluent has, at most, 10 ft to traverse to the sensitive volume of the analyzer. At the recommended operating rate of 150 cm^3/min , the maximum residence in the tertiary loop, including the analyzer itself, is 2.5 sec.

The total system is thus capable of delivering effluent to the sensitive volume of the analyzer within 10 sec (2 sec + 5.5 sec + 2.5 sec) after leaving the radiation field.

Except for brief periods at startup (38 min @ 1 Mw and 34 min @ 2 Mw), the reactor was operated at 3-Mw thermal power throughout the test. The average corresponding exposure dose rate for the liquid hydrogen was 2×10^9 ergs/gm(C) hr, and the average neutron flux (neutrons of energy greater than 2.9 Mev) was 2.4×10^{11} n/cm² sec. The diagram below summarizes a sample history from introduction into the dewar until the measurement was made.



$$DR(\text{avg}) = 2 \times 10^9 \frac{\text{ergs}}{\text{gm(C) hr}}$$

$$\phi(\text{avg}) = 2.4 \times 10^{11} \text{ n/cm}^2 \text{ sec}$$

Briefly, the AGPGAS was put "on stream" as soon as LH₂ was admitted to the system, and was continuously monitoring the effluent throughout the course of the test except during periods when the system was unattended. During those periods, bottled hydrogen gas was put through the analyzer in order to prevent bridge-element burnup. This procedure permitted bridge power to be left on at all times, and measurement could be resumed by merely valving bottle gas off and effluent gas on.

The RTT test-plan called for periodic reactor retractions and LH_2 flow terminations, which it was hoped would also prove valuable to the conversion measurement. This did not turn out to be the case, however, because of the very low effluent rate when the radiation field was simultaneously withdrawn with LH_2 flow terminations.

About one-fifth into the test, it was necessary to shut down the reactor for 5 hr in order to conserve LH_2 . The shutdown and the subsequent restart amounted to a repetition of the test, permitting confirmation of earlier behavior.

4.4 Results

4.4.1 Maximum Conversion

The maximum conversion measured was 3% (97% parahydrogen reduced to 94%). Losses in the fill line were estimated from dewar boil-off rate data as 15%. Fill-line losses represent a diluent; therefore, the actual conversion is believed to be $3\frac{1}{2}\%$.

4.4.2 Rise Time

Ortho concentration did not jump to the steady-state level, but rose slowly with time. There was no discernible increase in ortho content for the first 80 min. From startup plus 80 min to startup plus 120 min, the ortho concentration increased $\frac{1}{2}\%$. From startup plus 2 hr to startup plus 5 hr, the ortho increased almost linearly from $\frac{1}{2}\%$ to 3%, where it stabilized.

4.4.3 Radiation Dependence

During the 5-hr unscheduled reactor shutdown, the ortho concentration returned to the level of the supply (3%). After the restart, the ortho concentration again climbed 3% to the 6% level.

Further indications of this radiation dependence were apparent during the LH₂ flow termination and reactor retractions that were a part of the RTT data-taking procedure; however, the procedure cycle was of insufficient time (for fear of barring the RTT's) to obtain definitive results.

4.4.4 Dewar Charge-Rate Dependence

During the very high use-rate period immediately preceding the unscheduled shutdown, the indicated orthohydrogen concentration due to conversion varied between $\frac{1}{2}$ % and 1%. These results are consistent with estimates that the average LH₂ use rate for this period was about twice normal.

After steady state was reached (at normal LH₂ flow rates), minor fluctuations in ortho concentration of $\pm .5\%$ maximum were observed to have the same average period as the pneumatic value automatically controlling the dewar liquid level.

Overcharging the dewar, which yielded a very high flash-off, caused indicated ortho concentration to approach that of the supply. When the overcharge was terminated, the indication quickly (~ 3 min) returned to the steady-state value.

4.5 Conclusions

Two findings of this test are believed to be most important:

1. There was a significant, measurable increase in ortho-hydrogen concentration - an increase that is demonstrably related to nuclear radiation.
2. This increase seems to be associated in some manner with the liquid phase, although the actual conversion may occur only in the gas phase.

In conclusion, it appears that radiation-produced species capable of causing para-to-ortho conversion are introduced into the liquid through interaction of the impinging radiation with the liquid itself, the objects immersed therein, and the walls of the containing vessel. These species are relatively long-lived and their concentration builds up to some level principally determined by the half-lives of the species, the radiation intensity, and the boil-off rate. Significant conversion probably does not occur in the liquid because the ortho energy levels are prohibited by the prevailing temperature. The conversion-causing species are "boiled off," along with the other constituents, and are then able to cause conversion in the higher-temperature-evolved gas.

NPC 24,397
31-8651

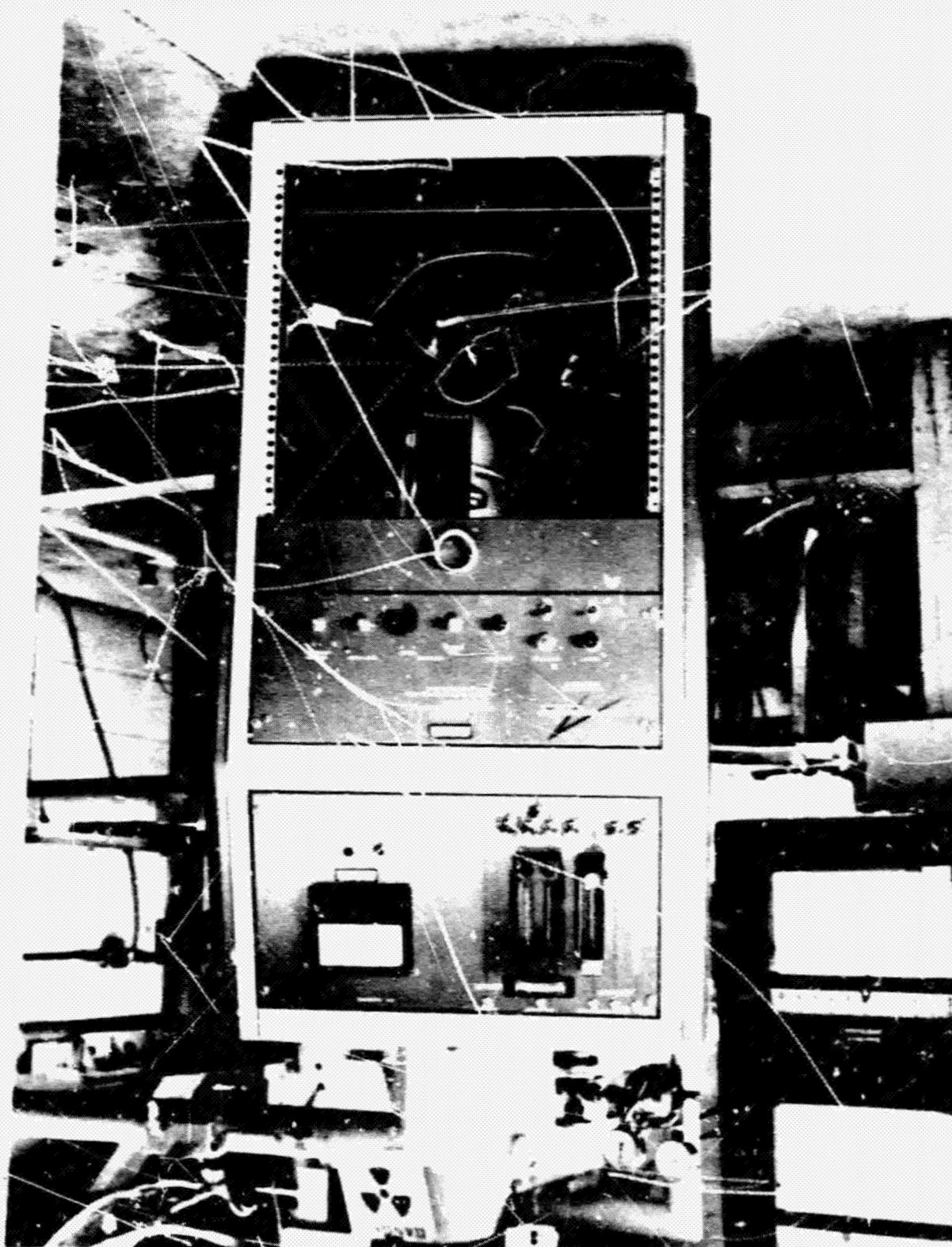


Figure 4-1 Apogee General-Purpose Gas-Analysis System (AGPGAS)

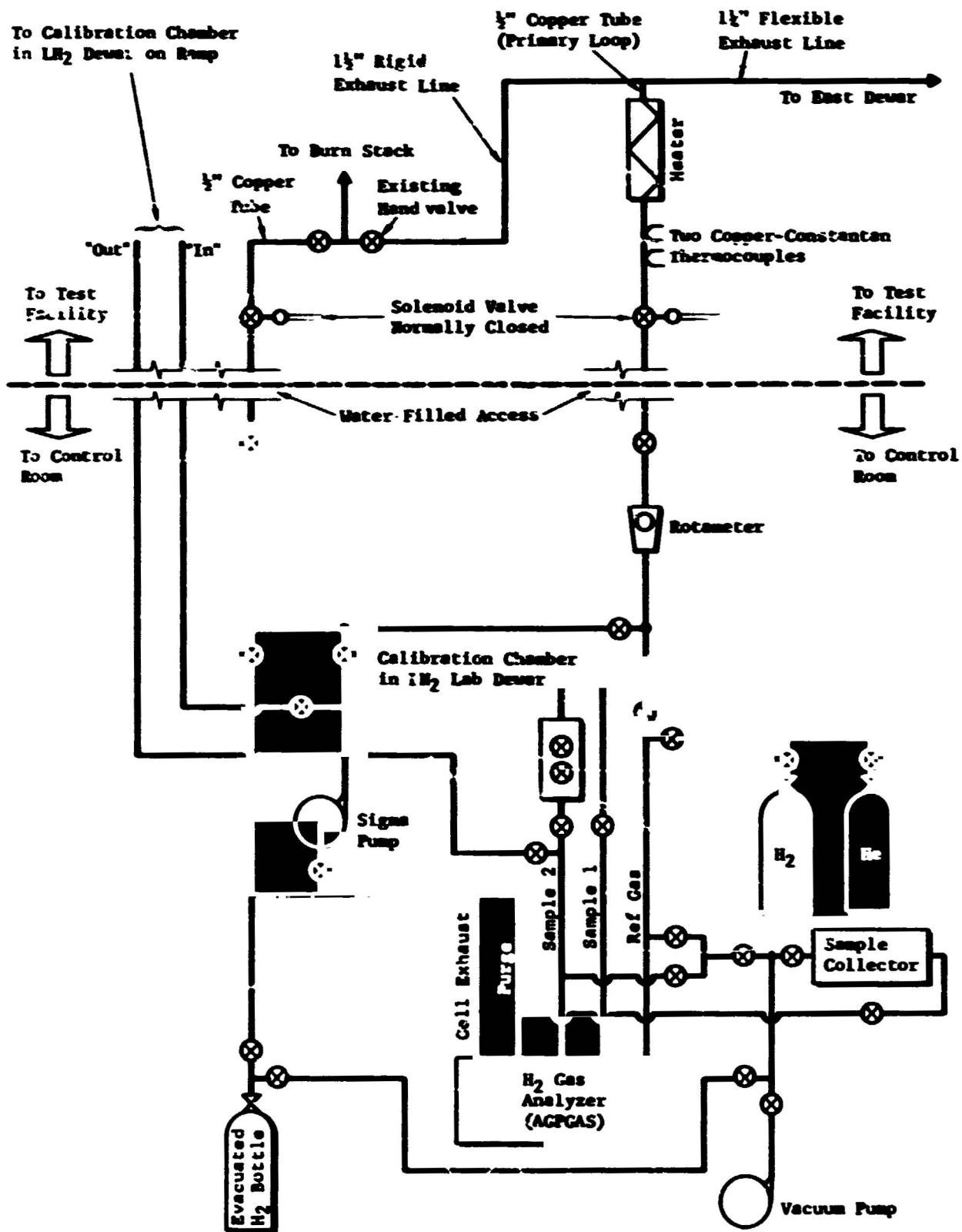


Figure 4-2 Schematic of Effluent Gas Sampling System

APPENDIX A

GTR RADIATION EFFECTS TESTING SYSTEM

The GTR Radiation Effects Testing System is located in the Reactor Operations Area at the north end of the NARF complex. Figure A-1 is a plan view and Figure A-2 is a cutaway view of the system. Figure A-3 is a close-up of the irradiation test cell and the reactor tank. During operation, the reactor is moved into the closet-like structure built into the north wall of the GTR tank. Items to be irradiated can be located on the north, east, or west sides of the closet, as indicated in the figures.

The reactor closet is constructed of 1-in. aluminum plate and partially covered by $\frac{1}{2}$ -in.-thick boral to attenuate thermal neutrons. The boral extends 36 in. east and west from the closet, along the tank wall, and 35 in. up and down from the horizontal centerline of the reactor core. The centerline is 57 in. above the test-cell floor.

The Ground Test Reactor (GTR) is a heterogeneous, highly enriched, thermal reactor that utilizes water as neutron moderator and reflector, as radiation shielding, and as coolant. Maximum power generation is 3 Mw. The GTR, in an aluminum enclosure to facilitate cooling-water flow, is suspended by

an open framework that is carried on a horizontal positioning mechanism at the top of the reactor tank. This mechanism permits the reactor to be positioned at distances ranging from 2 to 87 in from the north face of the closet.

Adjacent to the north wall of the irradiation cell is the handling area. Equipment permanently installed in the handling area includes a General Monitor explosive-mixture detection system and environmental conditioning equipment for the GTR Radiation Effects Testing System.

An integral part of the GTR testing facility is the shuttle system used to move test assemblies into irradiation position. This system consists of cable-driven dollies mounted on three sets of parallel tracks. The tracks extend from the irradiation positions adjacent to the reactor closet, up an incline to the north wall of the irradiation cell, and to a loading area on the ramp just north of the handling area. The system can be operated from either the control room or the dolly motor-drive shed on the north ramp. Full-coverage televiewing of the entire shuttle system is provided by means of closed-circuit television in the control room.

The control room (Fig. A-1) is a below-grade, reinforced concrete structure adjacent to the GTR system. The control room provides a shielded area for reactor instrumentation, control consoles, and test systems as well as special test equipment needed to conduct radiation experiments.

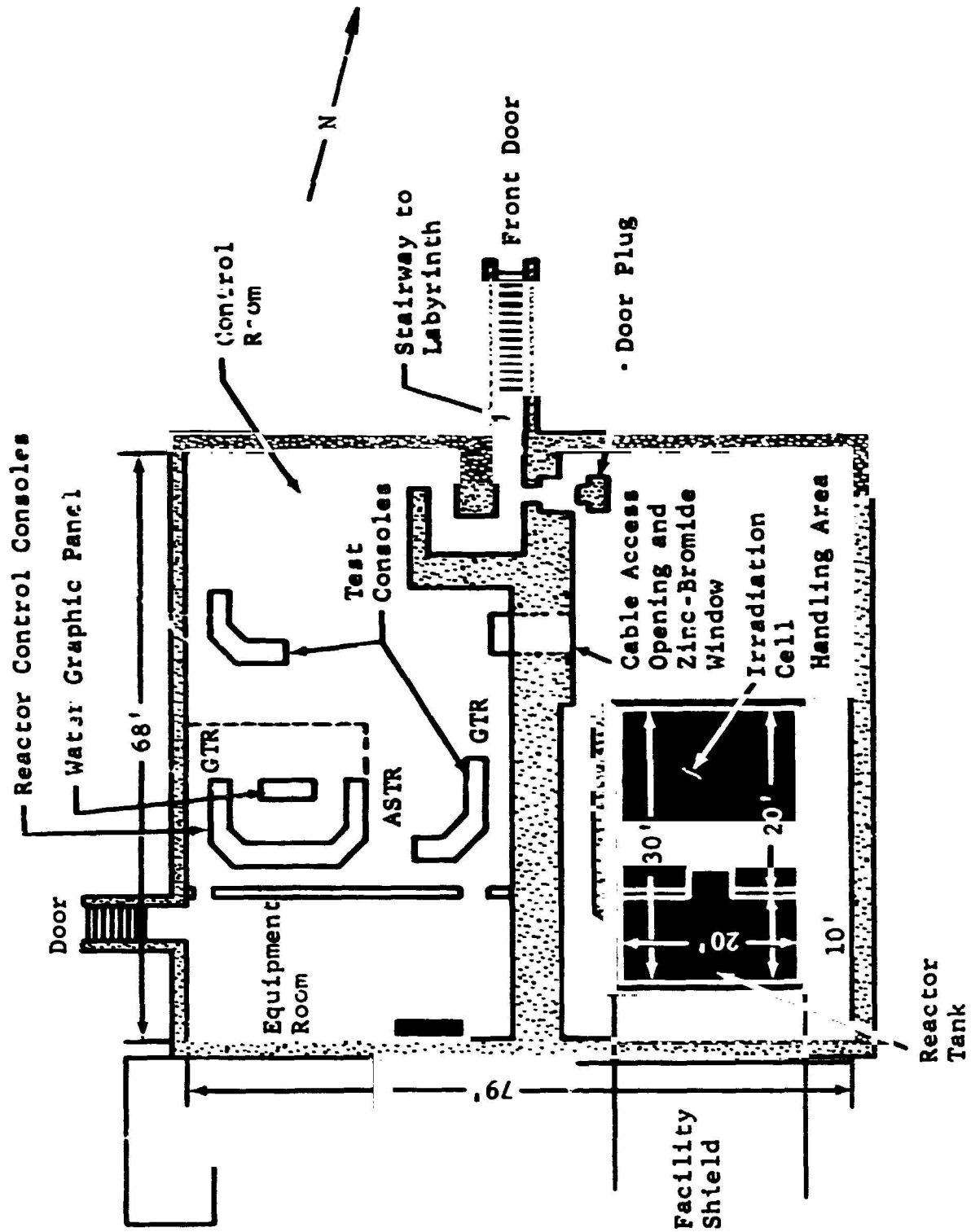


Figure A-1 Plan View of GTR Radiation Effects Testing System and Adjacent Reactor Control Room

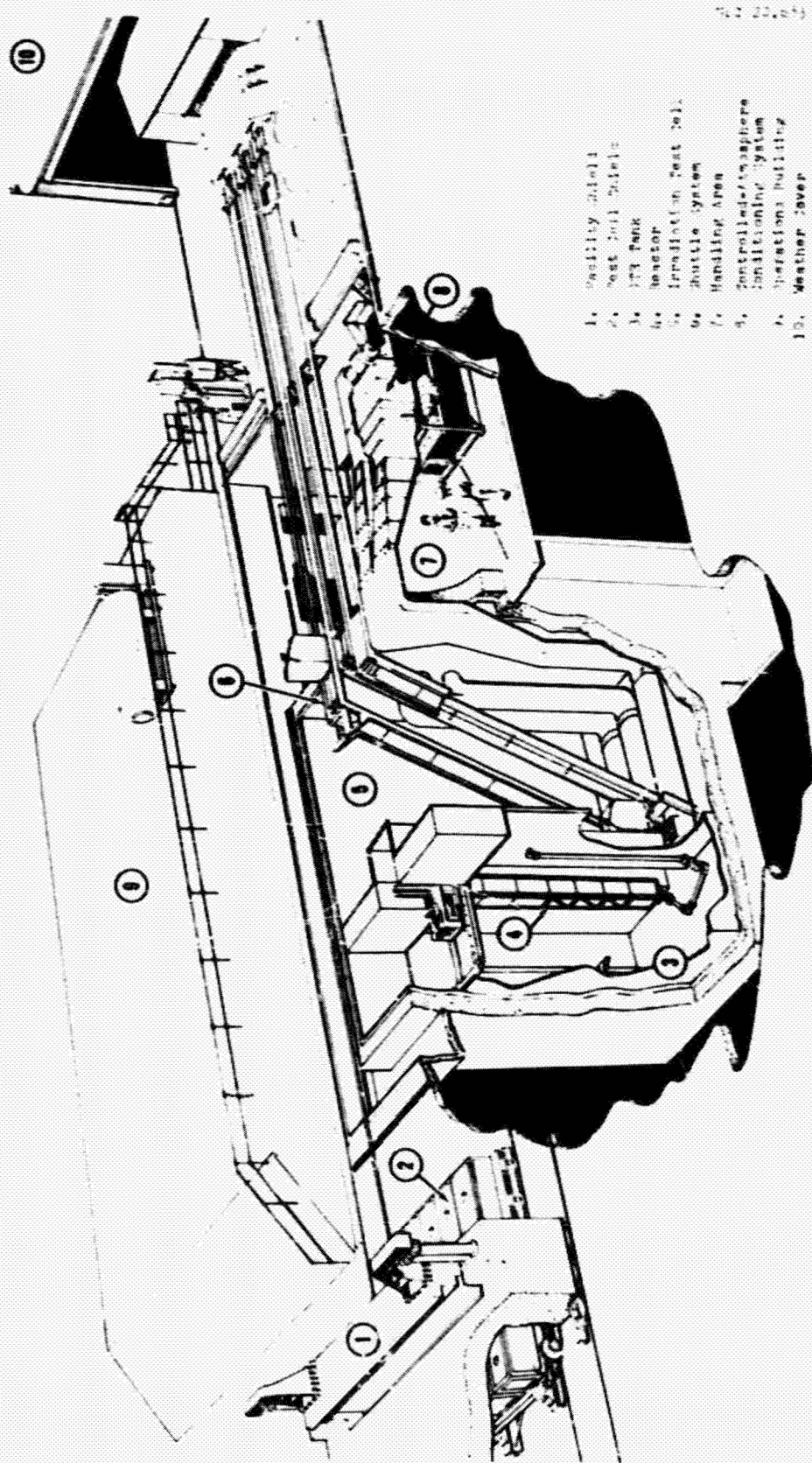


Figure A-2 Cutaway View of GTR Radiation Effects System

NPC 20,669
31-7909



Figure A-3 Irradiation Test Cell and Reactor Tank

BLANK PAGE

APPENDIX B

DOSIMETRY TECHNIQUES AND DATA

B.1 Nuclear Measurements

Nuclear measurements were obtained from dosimetry packets attached near the test components. Each packet consisted of a 3- by 3½-in. aluminum plate with the following detectors attached:

- One sulfoxy pellet for measuring fast-neutron ($E > 2.9$ Mev) integrated flux;
- Two phosphorous pellets (one bare, one cadmium-covered) for measuring thermal-neutron ($E < 0.48$ ev) integrated flux; and
- One nitrous-oxide dosimeter for measuring gamma dose.

In Section B.3 are presented figures showing the dosimetry packet locations; unless noted otherwise, the locations are viewed from the reactor. The dosimetry readouts for the packets are given in Table B-1. Table B-2 gives the radiation exposure for each individual RTT. The values for neutron flux ($E > 2.9$ Mev) at the RTT positions were obtained from the dosimetry data contained in Table B-1. The gamma doses were then determined using neutron-to-gamma ratios established in previous experiments and mapping runs. The ratio of neutron flux with $E > 1$ Mev to that with $E > 2.9$ Mev has been established to be 2.8; this ratio was used to obtain values for neutron flux with $E > 1$ Mev, as shown in Table B-2.

Table B-1
Dosimetry Data (Measured)

Packet No.	Integrated Neutron Flux (n/cm ²)	
	E < 0.48 ev	E > 2.9 Mev
1	4.25(16)	2.43(16)
2	4.20(16)	2.60(16)
3	3.79(16)	2.24(16)
4	4.24(16)	2.48(16)
5	4.25(16)	2.60(16)
6	3.79(16)	2.35(16)
7	3.88(16)	2.19(16)
8	3.71(16)	2.64(16)
9	3.32(16)	2.50(16)
10	1.90(16)	5.90(15)
11	1.91(16)	7.68(15)
12	2.24(16)	6.98(15)
13	1.92(16)	6.58(15)
14	1.96(16)	8.29(15)
15	2.23(16)	8.18(15)
16	1.95(16)	6.36(15)
17	2.24(16)	8.18(15)
18	2.43(16)	8.35(15)
19	1.71(16)	4.67(15)
20	1.66(16)	5.96(15)
21	1.89(16)	5.80(15)
22	1.49(16)	4.93(15)
23	1.60(16)	6.04(15)
24	1.65(16)	5.93(15)
25	1.75(16)	4.64(15)
26	1.57(16)	4.82(15)
27	1.60(16)	4.32(15)

Table B-2

RTT Exposure

RTT		Integrated Neutron Flux (n/cm^2)		Gamma Dose	n/cm^2
No.	S/N	E > 1 Mev	E > 2.9 Mev	ergs/gm(C)	E < 48 eV
1	8927	5.26(16)	1.88(16)	2.3(11)	5.31(16)
2	12333	5.24(16)	1.87(16)	2.3(11)	5.29(16)
3	6317	4.34(16)	1.55(16)	1.9(11)	4.38(16)
4	12330	4.84(16)	1.73(16)	2.1(11)	4.89(16)
5	4092	4.34(16)	1.55(16)	1.9(11)	4.38(16)
6	12340	4.20(16)	1.50(16)	1.8(11)	4.24(16)
7	4094	5.07(16)	1.81(16)	2.2(11)	5.11(16)
8	4096	5.21(16)	1.86(16)	2.3(11)	5.25(16)
9	4104	4.98(16)	1.78(16)	2.2(11)	5.04(16)
10	6319	5.12(16)	1.83(16)	2.2(11)	5.18(16)
11	7365	5.38(16)	1.92(16)	2.3(11)	5.43(16)
12	9372	5.04(16)	1.80(16)	2.2(11)	5.09(16)
13	9371	4.96(16)	1.77(16)	2.2(11)	5.00(16)
14	9370	4.48(16)	1.60(16)	1.9(11)	4.52(16)
15	1667	5.01(16)	1.79(16)	2.2(11)	5.06(16)
16	1666	4.73(16)	1.69(16)	2.1(11)	4.78(16)
17	6149	4.68(16)	1.67(16)	2.0(11)	4.73(16)
18	4107	5.18(16)	1.85(16)	2.3(11)	5.23(16)
19	211	4.93(16)	1.76(16)	2.1(11)	4.98(16)
20	9373	4.90(16)	1.75(16)	2.1(11)	4.95(16)

B.1.1 Neutron

The sulfoxy pellets used for fast-neutron measurements were molded from Epon-828 epoxy resin. These pellets were developed for use in high-flux irradiations and are usable at temperatures ranging from -423° to $+450^{\circ}\text{F}$. The resin contains a curing agent, sulfonyl dianiline, having 12.9% sulfur by weight. Since the curing agent is bound to the resin in a chemical reaction, a uniform dispersion of sulfur is ensured.

Standard foil techniques were used in specifying the neutron field (Ref. 5). All foils were counted in the NARF Nuclear Measurements Facility, and the data reduced by an IBM 7090 digital-computer program.

The neutron-integrated-flux values appearing in Table B-1 of this report were obtained from readouts of the dosimeter packets located within the dewars.

B.1.2 Gamma

The gamma doses appearing in this report were determined empirically from previous measurements of the neutron-to-gamma ratio for the east position of the GTR for a like configuration and from the neutron flux measured during this experiment. The reduction of data for N_2O dosimeters used to measure gamma dose for this experiment is not yet complete, but it is assumed that gamma doses from the neutron-to-gamma ratio as described above will compare favorably with the N_2O dosimetry readings.

B.2 Analytical CTR Neutron Spectrum

The neutron spectrum (Ref. 6) of the GTR in a water moderator has been measured to be Maxwellian at thermal energies ($E < 0.48$ ev), approximately E^{-1} from about 0.5 ev to 0.1 Mev, and essentially a fission spectrum for higher energies. In Figure B-1, this spectral shape has been mathematically altered to account for the attenuation of the thermal flux by the boral surrounding the reactor in the dry-pool configuration. The resulting spectrum has been shown to represent the actual spectrum fairly accurately.

Flux measurements have been made in the thermal-, epithermal-, and fast-neutron energy ranges by use of a variety of thermal, resonance, and threshold detectors. Fast-neutron flux measurements ($E > 2.9$ Mev) made on the dry side with the boral in place agree with those made on the wet (tank) side. The measured thermal flux is in general agreement with that obtained by integration of the analytical curve shown in Figure B-1.

B.3 Dosimetry Data

Twenty-seven dosimetry packets were attached to the test assembly. The locations of these packets are shown in Figures B-2 through B-6. The dosimetry readouts for each packet is given in Table B-1. The radiation exposure for each individual RTT is given in Table B-2.

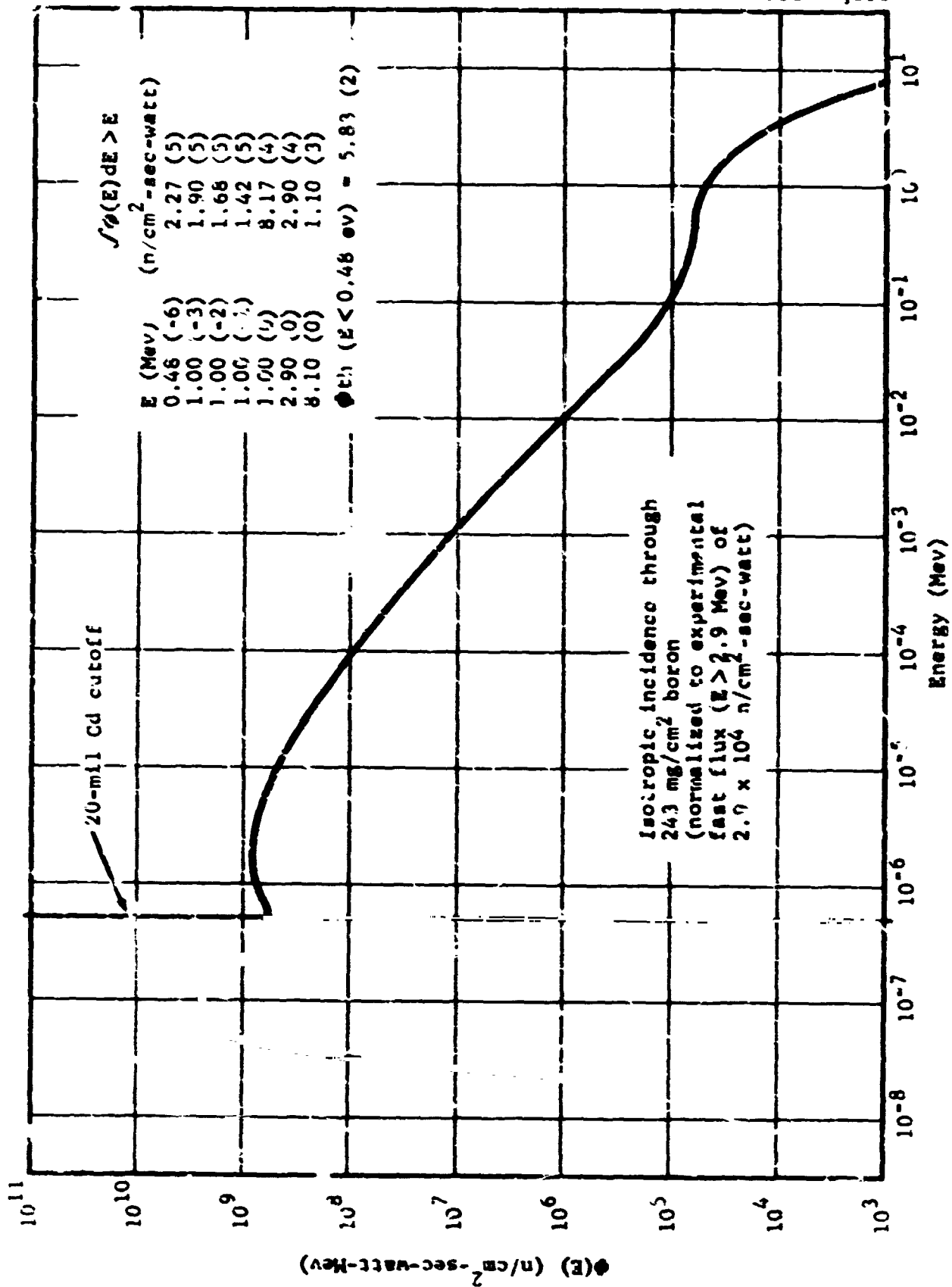


Figure B-1 Analytical GTR Neutron Spectrum

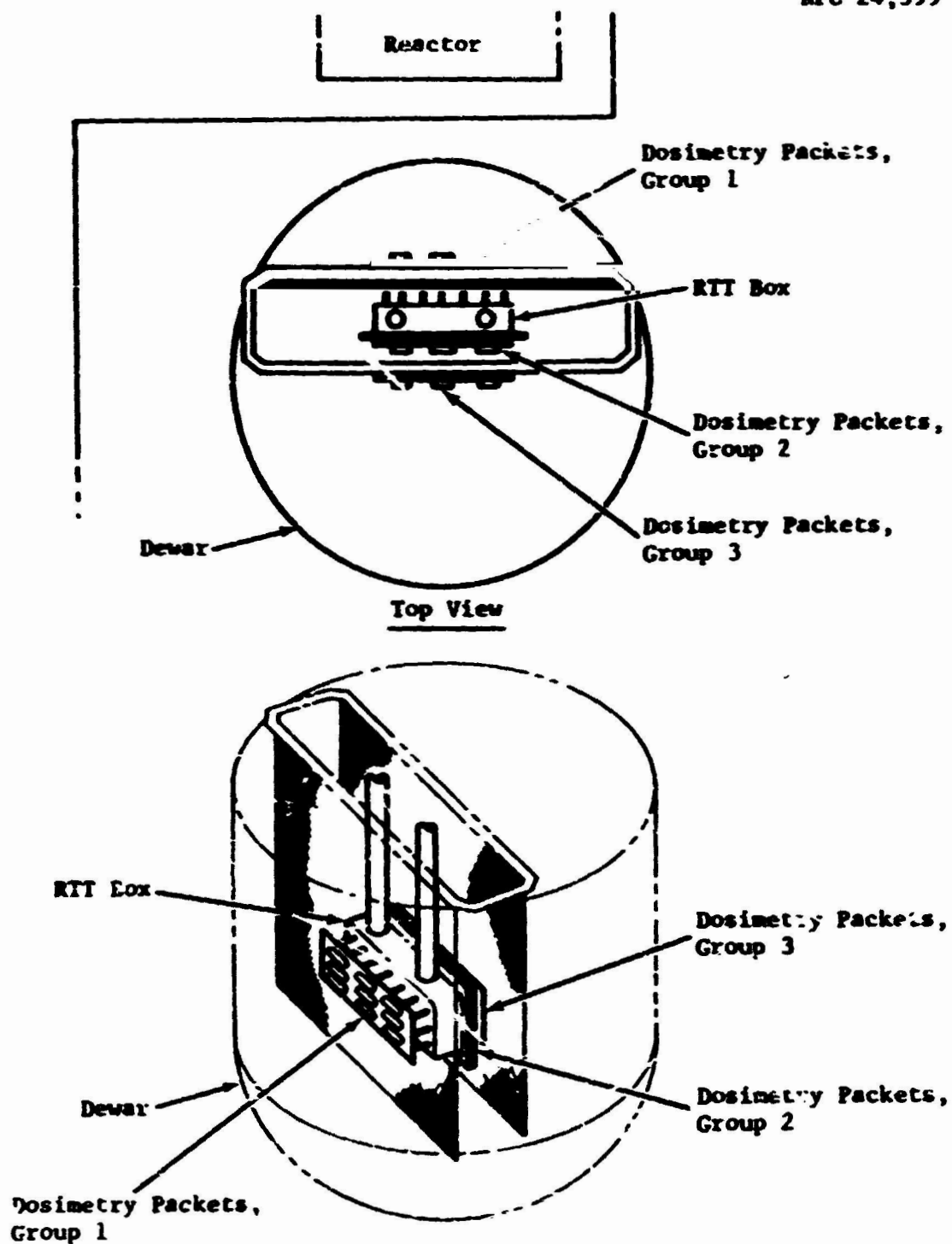


Figure B-2 Location of Dosimetry Packets

NPC 24,400
31-8672



Figure B-5 Location of Dosimetry Packets, Groups 1 and 3

NPC 24,401
31-8675

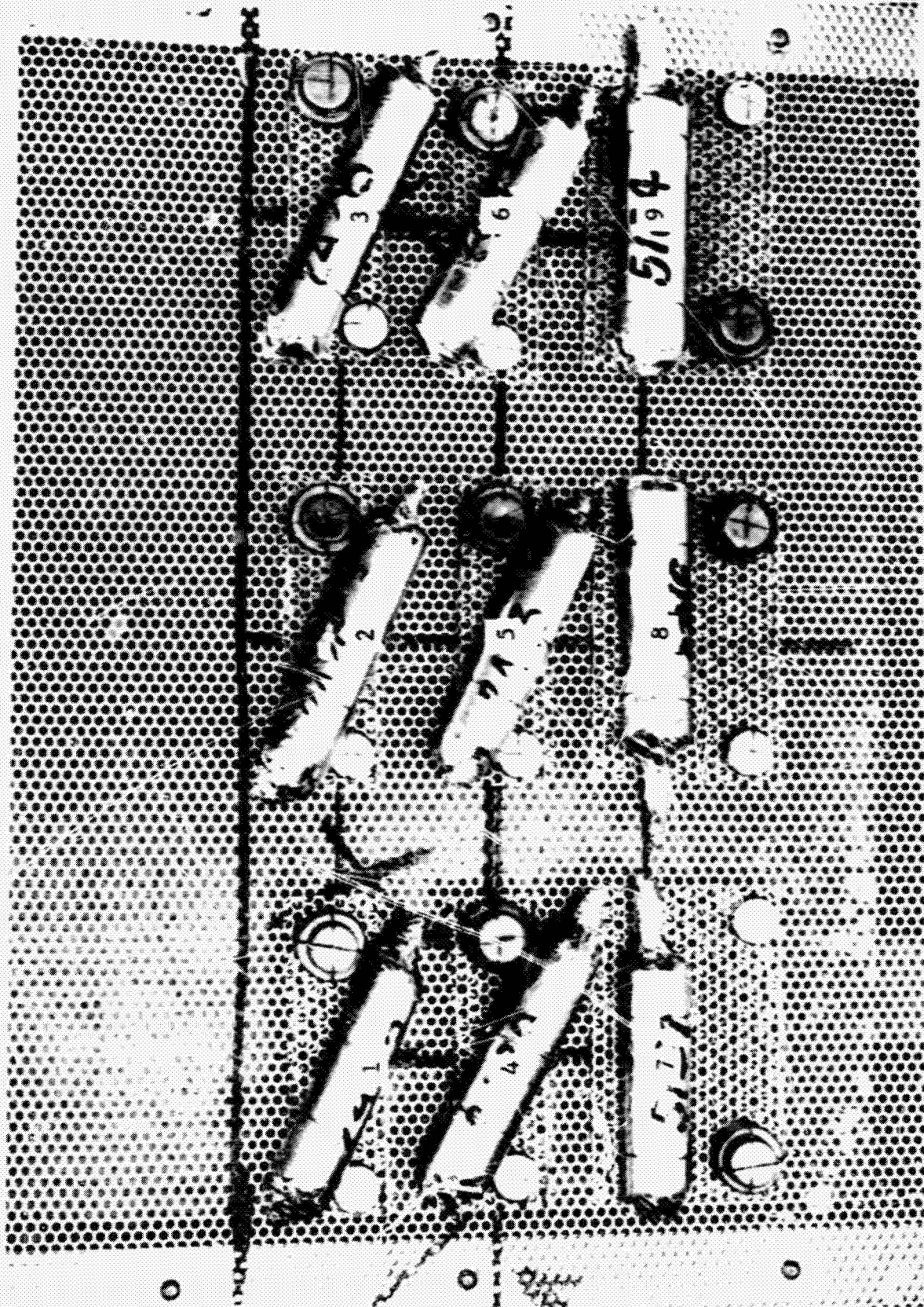


Figure B-4 Dosimetry Packets, Group 1, Viewed From Reactor

NPC 24,402
31-8673

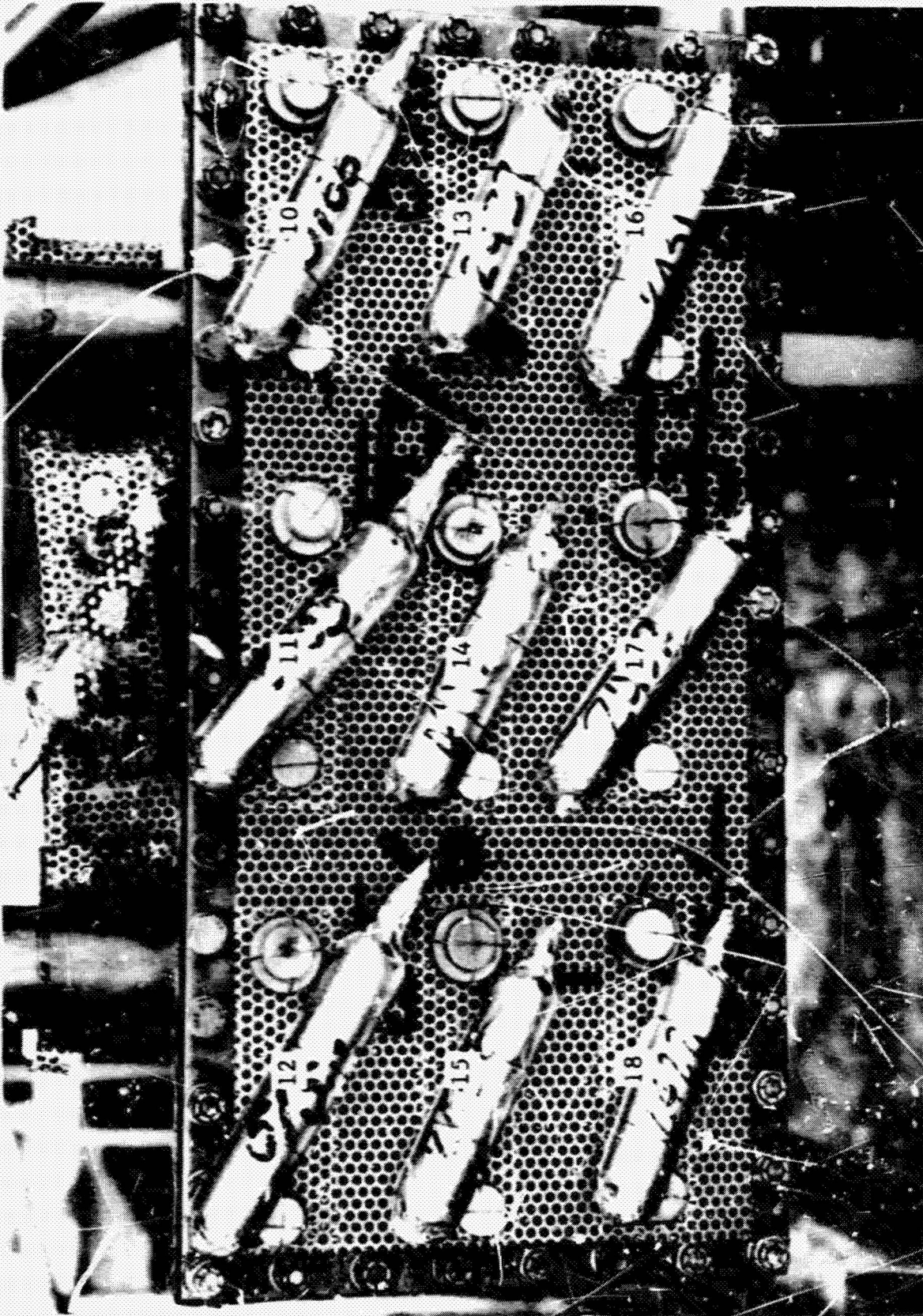


Figure B-5 Dosimetry Packets, Group 2, Facing Away From Reactor

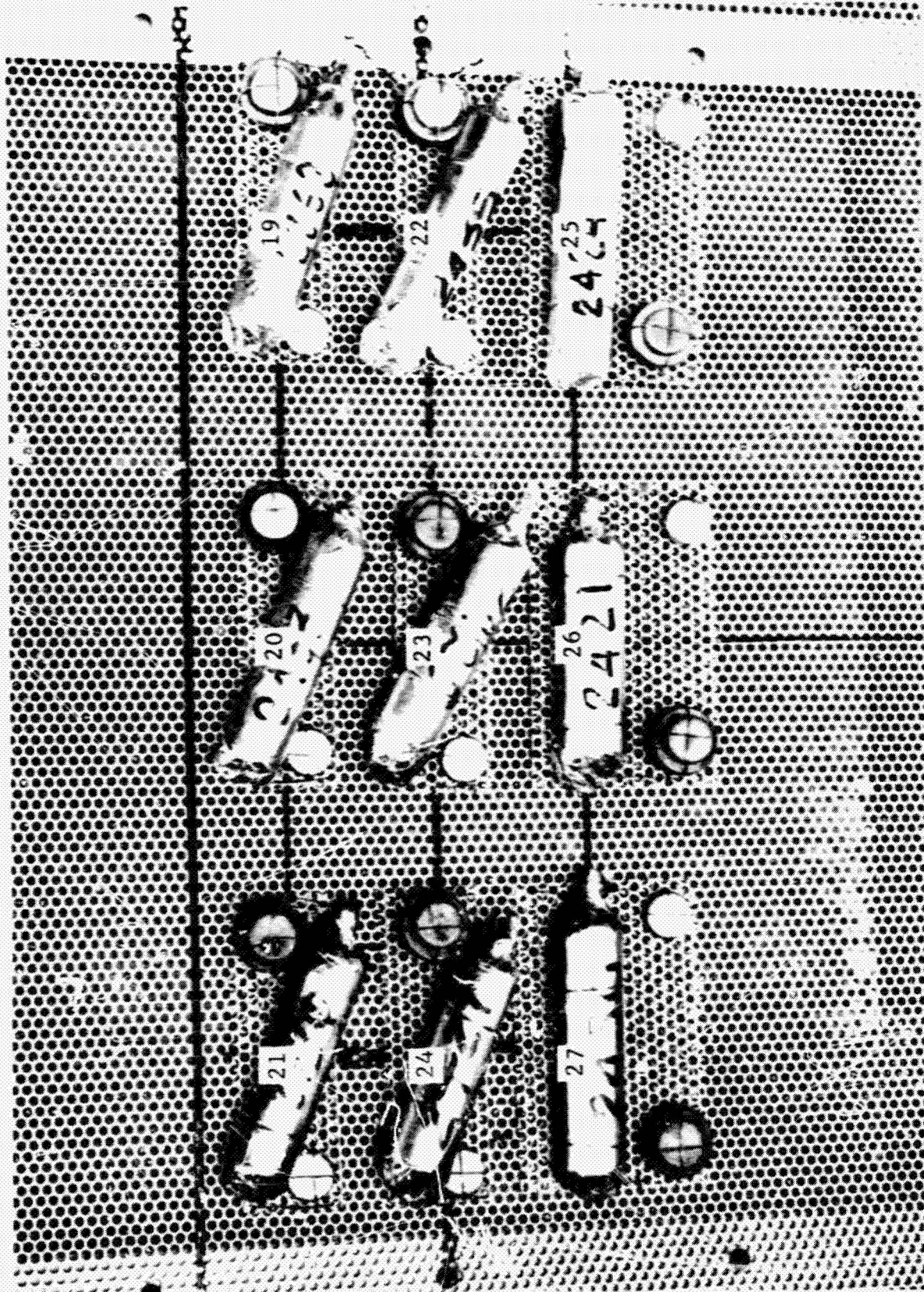


Figure B-6 Dosimetry Packets, Group 3, Facing Away From Reactor

BLANK PAGE

APPENDIX C

EXCERPTS FROM REACTOR OPERATIONS LOG

<u>Date</u>	<u>Time</u>	<u>Comment</u>
22 June	2354	Reactor to 1 Mw
23 June	0032	Reactor retracted
	0125	Reactor to 2 Mw
	0159	Reactor retracted
	0208	Reactor to 3 Mw

The reactor remained at 3 Mw except during periods incident to the following retractions:

<u>Date</u>	<u>Time Retracted</u>	<u>Duration of Retraction (min)</u>
23 June	0317	9
	1019	8
	1711	5
	2303	8
24 June	0503	11
	1113	14
	1709	27
	1809	Reactor shut down
25 June	(Reactor back to 3 Mw at 2346)	
26 June	0604	4
	1004	9
	1606	6
	2202	5

<u>Date</u>	<u>Time Retracted</u>	<u>Duration of Retraction (min)</u>
27 June	0406	4
	1019	3
	1602	4
	2204	4
28 June	0406	6
	1008	8
	1602	4
	2202	4
29 June	0403	6
	1004	7
	1358	4
	1758	4
	2159	3
30 June	0158	5
	0558	6
	0958	5
	1358	5
	1413	4
	1611	11
	1758	5
	2158	4
1 July	0159	5
	0558	36

<u>Date</u>	<u>Time Retracted</u>	<u>Duration of Retraction (min)</u>
1 July	0958	4
2 July	2031	Shutdown (end of test)

REFERENCES

1. Final Test Specification for GTR Irradiation Test No. 18, Aerojet-General Corporation Report No. RN-S-0299 (May 1966).
2. NARF Facilities Handbook, General Dynamics/Fort Worth Report FZK-185A (March 1964).
3. Burtnett, R. L., et al., NERVA Components Irradiation Program, Volume 6: GTR Test 15, General Dynamics/Fort Worth Report FZK-184-6 (19 March 1965).
4. Weber, L.A., et al., "The Vapor Pressure of 20°K Equilibrium Hydrogen," Cryogenics 2 (June 1962), 236-238.
5. Dungan, W.E., and Lewis, J.H., Nuclear Measurement Techniques For Radiation Effects Environment Testing, General Dynamics/Fort Worth Report FZK-9-175 (NARF-60-4T, 31 March 1963).
6. Dungan, W.E., Specification of the Neutron Flux in the Radiation Effects Testing Facility, Convair-Fort Worth Report MR-N-270 (NARF-60-23T, July 1960).
7. Farkas, Adelbert, Light and Heavy Hydrogen, Cambridge University Press, Cambridge, Mass., 1935.
8. Carter, H.G., Energy Storage Mechanisms in Liquid Hydrogen, General Dynamics/Fort Worth Report FZK-9-180 (NARF-62-15T, 31 October 1964,
9. Purcell, J.R., Draper, J.W., and Weitzel, D.H., "A Unique Thermal Conductivity Gas Analyzer," Advances in Cryogenic Engineering 3 (1960), 191-195.
10. Weitzel, D.H., Hershey, R.H., "Continuous Analysis of Ortho-Para Hydrogen Mixtures," Advances in Cryogenic Engineering 1 (1960), 122-125.